Fiber optimization of a carbon windsurfing boom

FEM fiber optimization for mass and stiffness

N. Huisman 4332059

Master of Science Thesis

TU Delft Delft University of Technology

Department of Offshore Engineering

Fiber optimization of a carbon windsurfing boom

FEM fiber optimization for mass and stiffness

Master of Science Thesis

For the degree of Master of Science in Offshore and Dredging Engineering, specialisation Bottom Founded Offshore Structures, Arctic and Wind at Delft University of Technology

N. Huisman 4332059

November 28, 2019

Graduation Committee:
Prof.dr.ir. A. Metrikine
Ir. C. Keijdener
Dr.ir. M. Pavlovic

Faculty of Mechanical, Maritime and Materials Engineering (3mE) · Delft University of Technology

Abstract

The goal of this research is to optimize the fiber layup of a carbon windsurfing boom for weight and stiffness. A windsurfing boom should be stiff to provide an efficient basis for the energy transfer from the sail through the surfer to the board. The weight of the boom is important as the total weight of the rig influences the performance, especially during movements where the swing weight of the rig is important.

To optimize the fiber layup the FEM simulation software of SolidWorks is used. This software allows the user to divide the part in sections and specify the layup per section in terms of orientation, thickness, and material. The output of the FEM simulation is the mass and the displacement under different load cases. The load cases are based on an experiment where the loads during sailing are determined with load cells and strain gauges. The FEM simulation is validated and scaled based on two experimentally determined force-displacement relations. The FEM is scaled with the force-displacement relation of the first loading point by scaling the given material parameters by 0.78. The FEM is then validated with the force-displacement relation of the second loading point.

New fiber layups are generated based on stress direction, previous iteration results, and engineering intuition. The mass and displacement are the evaluation criteria as the highest stress is much lower than the critical stress.The 50 new generated layups and their respective mass and displacement results are evaluated with a performance equation to determine which layup has the highest performance for the combination of mass and displacement. The coefficients in the performance equation are chosen so that both parameters have equal weight. The chosen layup is further evaluated with a required fiber overlap section.

Two booms with the new layup are evaluated with the same experiment that is used to validate and scale the original FEM. At the first loading point, where the main loading during sailing is applied, the new layup is 16 percent stiffer than the original layup, as predicted by the FEM. The experiment results for the second loading point showed that the new layup was 5.5-7.5 percent stiffer than the original layup instead of the predicted 13 percent. This difference is due to the straight tubes that are glued to the end of the optimized boom body which are made by a different manufacturer. Changing the stiffness of these tubes makes the FEM results converge to the experimentally determined values. The experiment results of both

layups are evaluated with the performance equation as the stiffness has increased but the mass has increased from 2.19 to 2.25 kg as well. The performance equation showed that the new layup outperforms the original layup for both loading points. The project goal to optimize the layup for mass and stiffness is therefore achieved. For the layup of the boom, a sandwiched layup of unidirectional fibers with biaxial fibers at the in- and outside of the circular cross-section was determined as the best performing layup for the sections loaded under bending. For sections that are loaded under both torsion and bending additional layers of biaxial fibers were added at the inside of the circular cross-section. These biaxial fibers are added at the inside as the unidirectional fibers are used at the outside to create the largest moment of inertia for these fibers as the displacement due to bending is leading in this case. Even the small translation of fibers from the inside to the outside of the layup can make a significant difference.

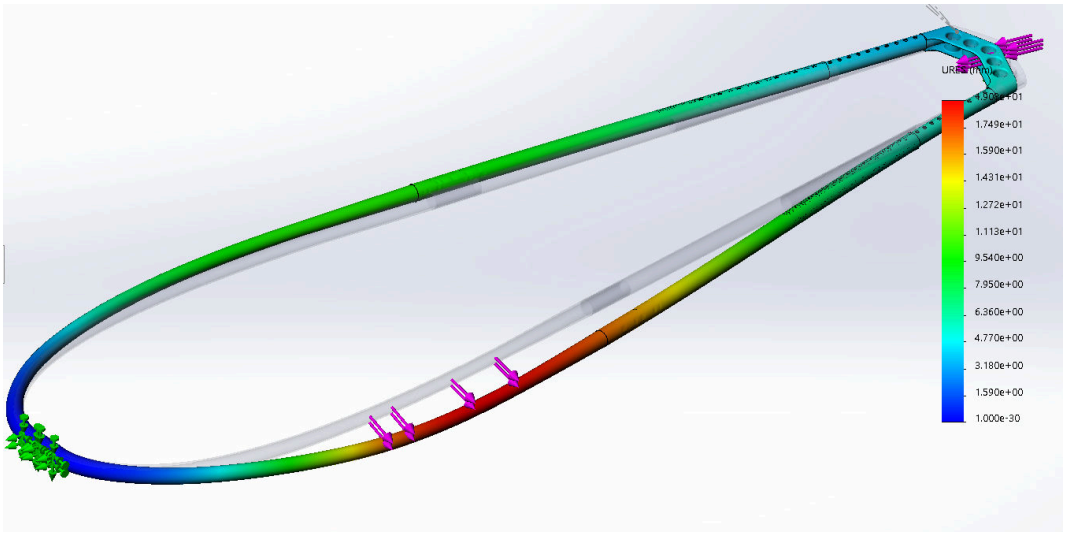

Figure 1: FEM simulation under full loading

Table of Contents

List of Figures

List of Tables

Preface

Windsurfing, the most beautiful sport on earth. The freedom of flying over the water driven by the wind with the rattling sound of your board barely touching the water. It is this passion for windsurfing that initiated this project. Looking for the best performing equipment to maximise the performance during slalom races and free sailing I started to design and build custom windsurfing booms together with my friend Pieter Bijl. After one and a half year we made our own custom booms that were much lighter than its competitors on the market. Finding the best performing layup was an expensive and time consuming process and that is how the idea for this master thesis came to life. What if, instead of just building and testing booms with different layups, I could use a more scientific approach by measuring the loads and evaluate different layups with a FEM?

The master thesis you are holding is the final result of this idea. This report describes the entire process to determine the best layup, from measuring the loading to the evaluation of the new layup. By finishing this research, the last assignment for the master Offshore and Dredging Engineering with the specialisation Bottom Founded Offshore Structures, Arctic and Wind at the TU Delft is completed.

During this process I was lucky enough to get the help from different people. There are a few people I would like to thank in particular. Starting with my TU supervisor Chris Keijdener and the head of graduation professor Andrei Metrikine, first of all I would like to thank you for accepting this project as graduation project. Thank you for your help and feedback during the progress meetings and via email. Thank you dr. Marko Pavlovic for being part of the graduation committee and the valuable feedback and input I received during our conversations. Thank you Jos van Driel for supplying me with the required measurement equipment and helping me with setting up the water experiment equipment. Thank you Simon for helping me with the Arduino code when I was stuck. Thank you Gerard van Vliet and Rene van Ommen for the hospitality and help in your workshop and storing the steel experiment frame for more than half a year. Thank you all that are not named in this report but did help me in some way, really appreciated.

So there it is; the graduation report, I hope you enjoy reading it.

Delft, University of Technology
November 28, 2019

N. Huisman 4332059

Chapter 1

Introduction

This document is a report of a graduation project done on a carbon windsurfing boom. In this chapter a short introduction to the subject is given.

1-1 Introduction to a windsurfing boom

1-1-1 Introduction to windsurfing, boom components and loads

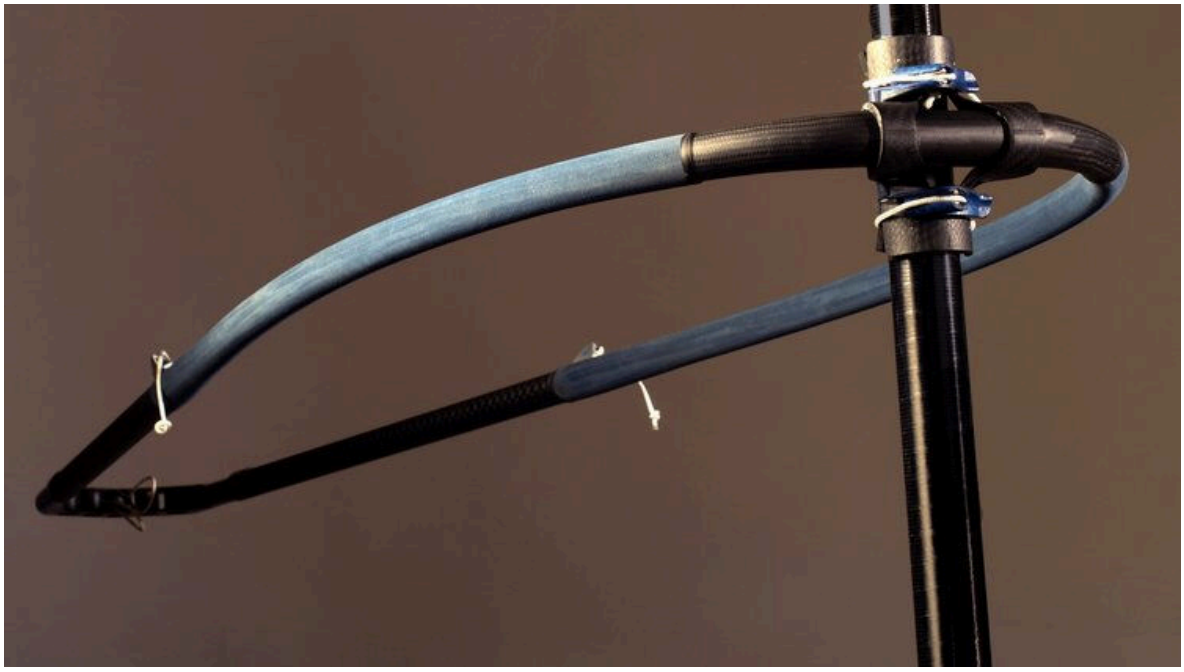

Figure 1-1: Carbon windsurfing boom

Figure 1-1 shows a carbon windsurfing boom, the subject of this report. This boom has been developed by the author of this report and has recently come to the market. Windsurfing is a water sport where a board with the surfer is driven by the power of the sail that is connected to the board, see figure 1-3. The boom, together with the sail and the mast, form the rig that generates power from the wind. The boom is the connection between the surfer and the sail, simply said the handles of the sail. With this boom the surfer is able to change the position of the sail and is therefore able to change the power output of the sail.

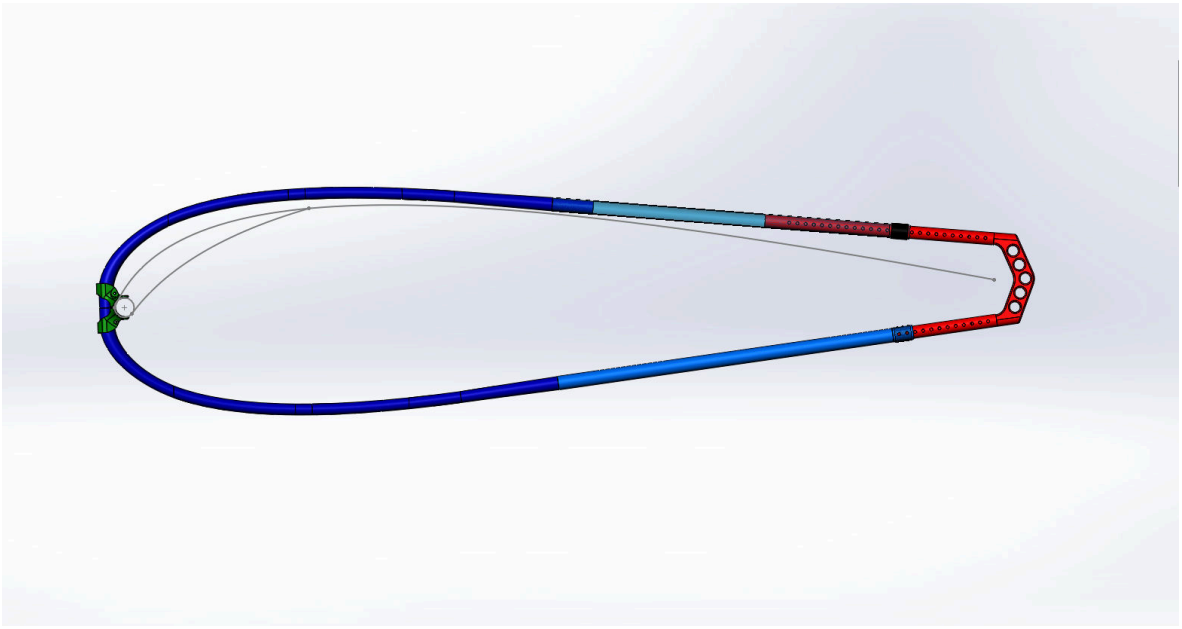

Figure 1-2: Boom parts

A windsurfing boom consists of multiple parts. An overview is given in figure 1-2 . The subjected windsurfing boom consists of a main body, highlighted in blue in figure 1-2. This main body consists of a curved section and a straight section. On this curved section straight tubes are glued, given in light blue. The main body is therefore made of three parts. This is done because a straight tube can easily and cheaply be made with a steel mandrel [3] in an autoclave. This has the advantage that this section can be made with industrial standards with known superior material properties. This has also the advantage that the inner diameter can be made with a high tolerance. This is needed because the tubes of the tail end of the boom, given in red in figure 1-2, slide into the body tubes as can be seen in the top side of the figure where the body tube is transparent. This sliding system provides the boom with the ability to be changed in length. The length is fixed with a double pin-hole system, the clip is given in black in figure 1-2. The boom is connected to the mast in the sail with the boom head, given in green in figure 1-2. The sail shape is given in grey in the figure. The clew of the sail is connected to the tail end with a rope and pulley system to the tail end.

The boom is the connection between the sail and the rider. The sail is inside the boom as can be seen in figures 1-2 and 1-3. The mast of the sail is inside the sail sleeve at the leading edge of the sail. The boom head is connected to the mast at the leading edge of the sail. At the trailing edge the clew of the sail is connected to the boom with a rope and pulley system. The loads on the boom are applied by the sail and by the rider who opposes the power of the

Figure 1-3: Windsurfing

sail. The main loading is transmitted through the harness lines (the red lines on the boom in figure 1-3, connected to the harness on the waist of the rider), given in red in figure 1-4. The secondary loading is transmitted at the clew of the sail, given in blue in figure 1-4. A third, smaller loading is transferred by the arms of the rider, given in green in figure 1-4.

A high performance boom should be light and stiff. The stiffness is important as the boom transfers the power of the sail through the surfer to the board. A stiff boom provides the basis for an efficient energy transfer. Furthermore the boom should be stiff as during gusts, where control becomes an issue, the boom tends to bend open allowing the sail to provide even more power, leading to even less control for the rider. Weight of the boom is also an important factor as a lower weight of the rig will potentially give more performance. This is due to, for instance, the reduced swing weight during maneuvers like gibing.

1-1-2 Startup of the Proboom project

This project all started with the desire to have the best equipment possible to win (inter)national slalom races. After some brain storm sessions the author and an ex professional slalom sailor, Pieter Bijl, decided to try to build a lighter and better boom. A new improved outline of the boom was designed and evaluated with an aluminum prototype. After recognizing the potential of this improved outline a high density foam mold was machined to produce a carbon boom. Approximately one and a half year later a new brand was born, Proboom. In these development years not only the outline of the main body was designed and

Figure 1-4: Loading applied to the boom

manufactured but also all other components such as the tail end and the boom head. This new boom has some innovative features and components that are now already being copied by the big brands. The key features of the Proboom are its low weight which is 18-42 percent lower than its competitors, the improved outline with a relatively small grip diameter which improves the ergonomics of the boom significantly, and the stiff connection to the mast due to the carbon boom head [4].

1-2 Fabrication process

1-2-1 Introduction to carbon fiber reinforced plastics

Carbon fibers are very small fibers that are composed of mostly carbon atoms [5]. The carbon fibers are bundled together after a both chemical and mechanical process to form a tow [6]. This tow can be used as a single tow or woven into a fabric. This single tow or woven fabric are both referred to as carbon fiber in this report. The thickness of the final tow is often expressed in a K number which stands for the number of filaments per bundle. A 3K fiber has therefore three thousand filaments per bundle and is therefore a thinner fiber than a 6K fiber which is composed of six thousand filaments per fiber. The thickness of a fabric is also often given in the weight per square meter. The carbon fibers are combined with an epoxy resin to form a composite with a very high strength to weight ratio. For the fabrication process of a carbon fiber reinforced plastic part three main methods are being used. A part can be made with prepreg carbon fibers. Prepreg stands for pre impregnated, which means that the fibers already contain the optimal amount of resin. The prepreg fibers are then cured in an oven, usually under pressure and/or vacuum, to obtain the optimal material properties [7]. Another production method is a Vacuum Infusion Process, VIP [8]. The layup is completed with dry fibers and the resin is infused with a vacuum. The most basic method is a wet layup.

This means that all fibers are manually wet during the layup of the fibers. Usually a vacuum is later applied to remove any excess of resin.

A carbon fiber reinforced plastic is usually not isotropic as the fiber is at its strongest in the direction of the fiber. Therefore a carbon fiber reinforced plastic is usually composed of fibers in multiple directions to optimize the fiber loading. A misalignment of the fibers will lead to a significant decrease in tensile strength and Young's Modulus [9][10]. This can also be seen in table 1-1 where the tensile strength and Young's Modulus are given for the used fibers in both 90 and 0 degrees orientation, where the 90 degrees orientation has much smaller values than the 0 degree orientation [11].

Table 1-1: Carbon fiber properties for Unidirectional fibers

Parameter	Value
Youngs Modulus 0°	135 GPa
Youngs Modulus 90°	10 GPa
In Plane Shear Modulus	5 GPa
Poisson's Ratio	0.30
Ult. Tensile Strength 0°	1500 MPa
Ult. Tensile Strength 90°	50 MPa
Ult. Comp. Strength 0°	1200 MPa
Ult. Comp. Strength 90°	250 MPa
Density	1.6 g/cm^3

For this project multiple fabrics are used. Table 1-2 gives the different used fabrics. The unidirectional fibers are fabrics with fibers that are parallel to each other. The bi-axial fabrics, referred to as biax in the report, are fabrics with fibers in two directions. If the used fabric is not deformed the angle between the two fiber directions is 90 degrees. This fabric is usually used to give medium bending strength and medium torsional strength. When used under 45 degrees this fiber gives high torsional strength.

Table 1-2: Used carbon fiber fabrics

Fiber weave	Gram per square meter
Unidirectional 6K sleeve	325
Braided bi-axial 6K sleeve	300
Braided bi-axial 3K sleeve	175
Unidirectional 6K fiber	300
Unidirectional 3K fiber	150

The first three fiber fabrics in table 1-2 are sleeves. This means that the fabric is woven as a sleeve. This is often used in circular parts to ensure the same wall thickness over the diameter. These sleeves can be used in both unidirectional and biax orientation. For the biax sleeves the angle between the fibers will change when the diameter of the sleeve is changed. Figure 1-5 gives an example of the carbon fiber sleeves.

Figure 1-5: Carbon fiber biax and unidirectional sleeves [1][2]

1-2-2 Fabrication process in the industry

Carbon booms are built with a solid outer mold and a soft tube as inner mold. The industry produces the carbon booms with prepreg carbon fiber. The prepreg carbon fiber plies are rolled around the inner tube and placed into the outer mold. The resin is cured under pressure in an autoclave to reach optimal material properties. The advantage of prepreg fiber, next to a clean and dry process, is that the ratio of resin to fiber is optimal as the resin is already in the fiber. The advantage of this method is that it is an easy process as the plies are rolled around the tube and then put into the mold. The curing is a fast process, and the production rate is therefore higher than for other production methods [12]. The main disadvantage is that the fiber orientation is harder to control as the fibers are rolled around the tube and then forced into the shape of the boom.

1-2-3 Fabrication process of the Proboom

For the boom of subject, vacuum infusion was chosen instead of production with prepreg carbon fiber. The reason to choose for vacuum infusion is that the layup of the fibers is easier and more flexible than for prepreg fibers. One of the challenges with prepreg fibers is to achieve a constant wall thickness over the diameter of the boom. This is due to the rolling of the fibers and the difference in diameter over the length of the boom, requiring more material in certain areas. By choosing for vacuum infusion the layup of the fibers is more flexible and for instance braided carbon sleeves can be used, which provide a constant amount of material over the diameter.

The solid outer mold is made from carbon and glass fiber to match the material properties with the product so that the thermal expansion properties of both the mold and the product are the same. The mold starts with a layer of gel coat, given in green in figure 1-6, followed with a layer of glass fiber, given in grey. The next layer is the first layer of carbon, given in red. This layer of carbon also forms the heating element of the mold. The carbon layer is connected to a power source and acts as a resistance providing the required heat for post-curing. The carbon layer is isolated on both sides with a layer of glass fiber to prevent conductivity to the

other carbon layers. After the glass fiber isolation layers several carbon layers, given in black, are implemented to get the required stiffness. After these layers the heat is isolated with a layer of cork, given in brown in figure 1-6. The mould is then build up further with carbon fiber and PVC sandwich material. The square parts on both sides of the circular product are the slots for the vacuum seals.

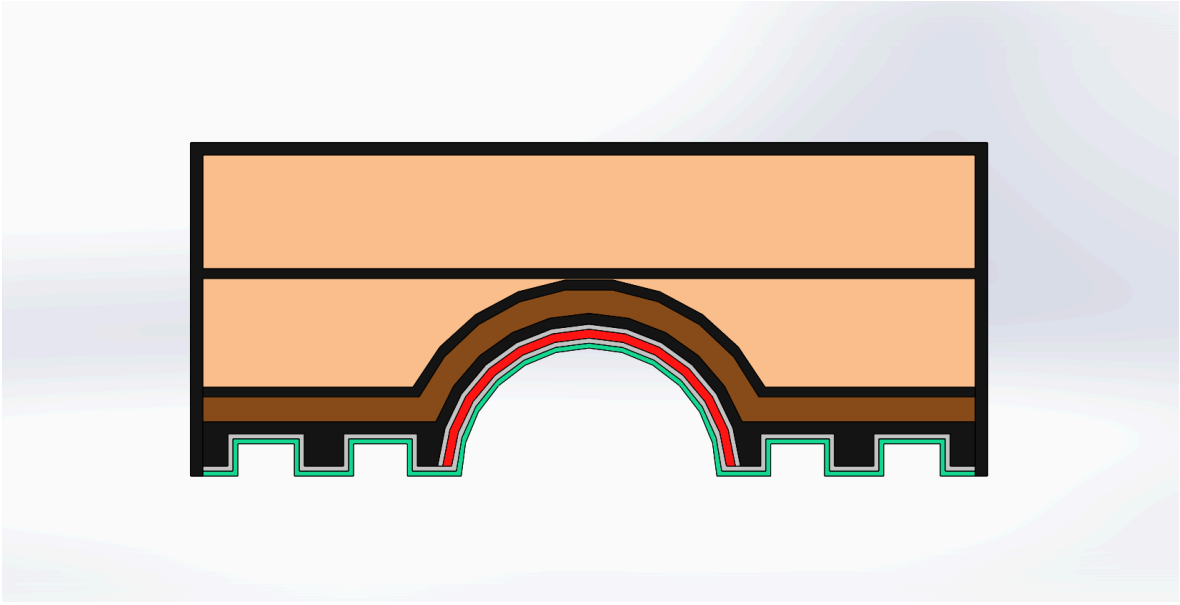

Figure 1-6: Schematic cross section of the mold

Figure 1-7 shows one side of the mold. The blue vacuum seal makes sure the product is under vacuum. The white vacuum seals form the vacuum chamber around the product. This is done to prevent air leaking into the product. If there is a leak in the blue seal it is still leaking into a vacuum.

The layup of the fibers is done by gluing part of the fibers into the solid outer mold, as can be seen in figure 1-7. This done with unidirectional fibers to reinforce the areas which require more wall thickness. The plies are cut at the edge of the mold so that the amount of material over the diameter of the boom is equal. The reason to glue these plies into the outer mold is that these plies can be glued on the exact required location which cannot be guaranteed with the carbon sleeves. The layup is completed with carbon sleeves, in both unidirectional and biax fibers, that are sled around the flexible inner mold, see figure 1-7. The layup of the fibers is limited by the curve of the boom and the change in diameter of the boom. The unidirectional plies are not able to make the full curve as the fibers on the outside of the curve should be longer than the inner fibers. The fibers in the unidirectional plies are held together with a very thin layer of glass, limiting the translation of a fiber with respect to the next fiber. The sleeves around the flexible inner mold are inserted in the mold at a smaller diameter. When the inner mold is pressurized the fibers are pushed to the walls of the outer mold. This requires a small translation of the fibers over the inner mold. However, due to the curve of the boom this translation is also limited. Therefore the layup is divided in three sections; two sections starting at each end of the arms of the boom, and one section in the front of the boom. This limits the maximum curve in each section allowing the fibers in the plies to translate to the required position. This division in sections means that a proper overlap

section between the sections is required. When the layup of the fibers is completed, the mold is closed and put under vacuum. The flexible inner mold, the tube, is pressurized (up to 6 bar) to push all fibers to the face of the outer mold, and to mimic the curing conditions in an autoclave. The resin is then infused by the vacuum system and cured inside the mold.

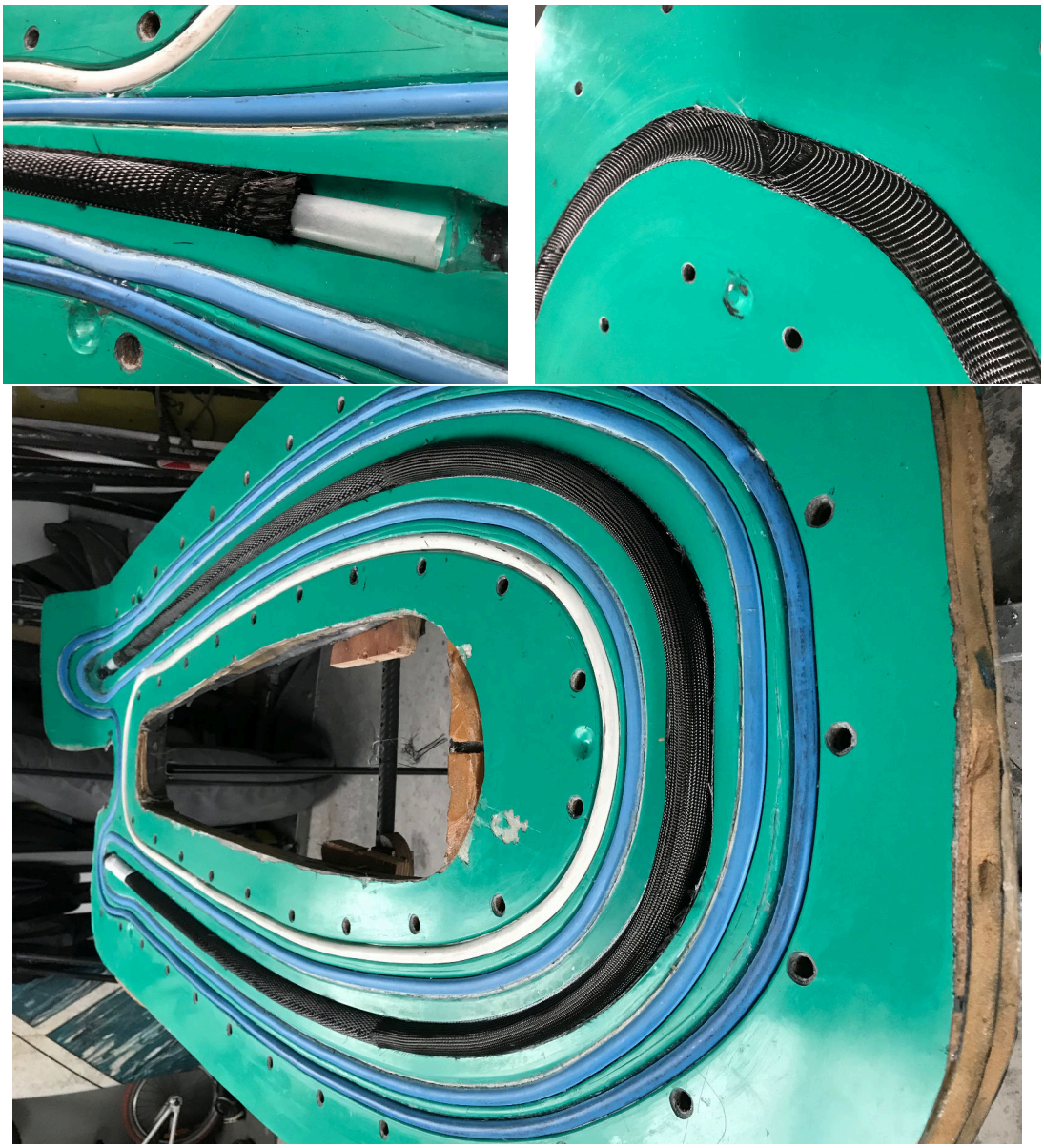

Figure 1-7: Production of the boom body with a solid outer mold and a flexible inner mold

1-3 Project goal

As already described in section 1-1, stiffness of a windsurfing boom is very important as is the weight of the boom. The stiffness of the boom can be changed by changing the layup of the carbon fibers, which also changes the weight of the boom. Therefore the goal of this project

is stated as: Optimize the fiber layup for a light weight and stiff carbon windsurfing boom. Both weight and stiffness can be measured and will be criteria to evaluate the performance of the different layups. The boundary condition to this project goal is that the boom will not fail under normal loading.

Chapter 2

Load Identification

In this chapter the loads that are acting on the boom are described and analysed. The loads on the boom should be known to provide a reliable basis for the fiber optimization. Different loads under different angles might lead to different optimal fiber layups. Therefore the loads that occur during sailing are measured and processed.

2-1 Boom loads

As described in 1-1 a windsurfing boom is the connection between the sail and the rider. The boom is connected to the mast and to the clew of the sail. The mast of the sail is inside the sail sleeve at the leading edge of the sail. The boom is connected to the mast with a boom head at the leading edge of the sail. At the trailing edge the clew of the sail is connected to the boom with a rope and pulley system. The loads on the boom are applied by the sail and by the rider who opposes the power of the sail. The loading of the sail is applied at the clew of the sail through the rope and pulley system. The main loading applied by the rider is transmitted through the harness lines that are connected to the harness of the rider. The secondary loading applied by the rider is transmitted by the back arm of the rider. The front arm does not apply a significant load as this arm is only used to keep the balance and control during straight line sailing. The loads during sailing are shown in figure 1-4. A schematic view of the loads where the load by the front arm of the rider is neglected is given in figure 2-1. The loads by the harness and the arm of the rider have an in plane and an out of plane component as can be seen in figure 2-2

2-2 Load identification experiment setup

2-2-1 Implementation of load cells and strain gauges

Figure 2-1 shows that there are three forces that need to be determined. The force applied by the sail, given in blue in the figures, is measured by use of a load cell. The load cell is

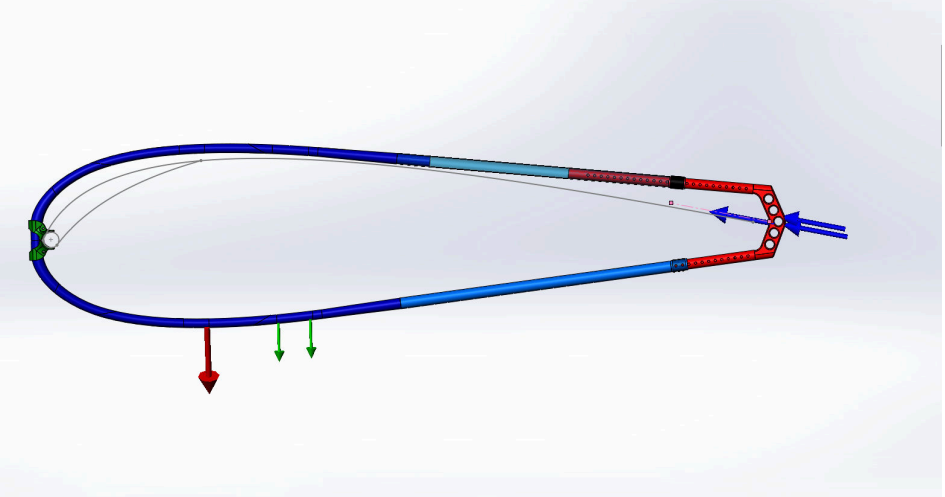

Figure 2-1: Schematic view of the loading on the boom

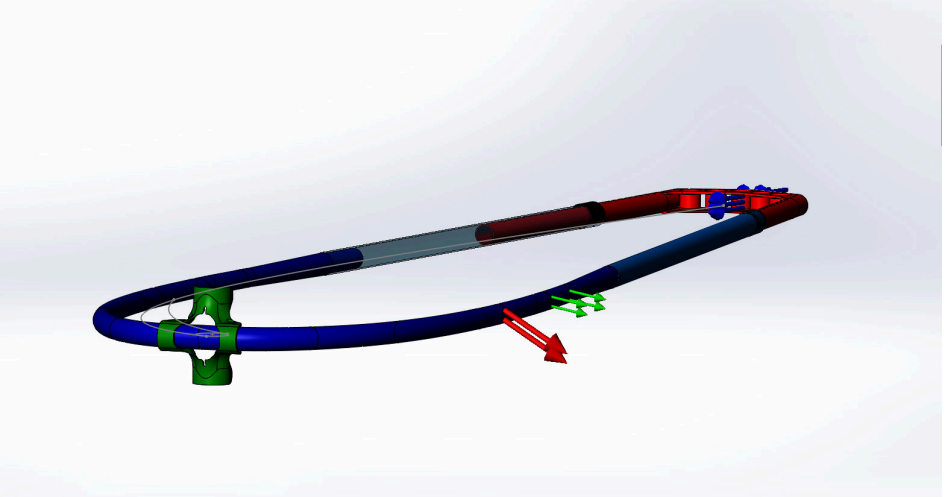

Figure 2-2: Loading angles

mounted on the sail and on this load cell the pulleys are mounted to keep the rope and pulley system similar to the normal system. To measure the load applied by the harness line, given in red in the figures, the harness line is replaced by a load cell with on each side a separate line to connect to the boom and to the harness. With this load cell the magnitude of the force can be determined but the angle is still unknown. The angle of the harness load and the magnitude and angle of the load applied by the arm of the rider is less straight forward to determine. To determine those, strain gauges are applied at the estimated point of maximum deflection of the boom in both horizontal and vertical direction. These strain gauges will not provide the exact angle or load applied by the arm of the rider but will give a representation of the total load on the boom exerted by all forces. With the measurements of the strain gauges the load applied by the arm of the rider and the angles under which they occur can be determined with further experiments. The experiment setup is shown in figure 2-3.

The strain gauges are applied in sets of two at the top and bottom for the vertical deformation and at the sides for the horizontal deformation. The sets of strain gauges are then coupled in a Wheatstone bridge circuit. This circuit is used to accurately measure the difference in resistance due to the deformation of the strain gauges. The Wheatstone bridge circuit is given in figure 2-4 [13].

The circuit consists of the four resistances given by the four strain gauges. Deformation of the strain gauges changes the resistance. To measure the difference a voltage is applied over the circuit, U_I in figure 2-4. The voltage measured between the Wheatstone bridge, U_O, is a measure for the change in resistance of the strain gauges [14]. The change of resistance can be related to the deformation and the applied loads. This same principle is also used in the load cells that are used to measure the clew and harness loads.

2-2-2 Sensor scaling and processing

As all measurements should be processed during sailing an Arduino is used to read out the sensors and process the data. The voltage difference that should be measured in the Wheatstone bridge has a very small magnitude and should therefore be amplified for accurate measurements. The signals from the sensors are therefore amplified by INA125 amplifiers. With these amplifiers and some chosen resistances the sensors are also scaled and calibrated for use in the boom.

The load cells are simply scaled by adding loads to find a voltage-load graph. The load cells are scaled with a chosen resistance to give values between 0 to 5 Volt in 1024 (Arduino) steps for a load ranging from 0 to 350kg.

The vertical strain gauges are scaled to give values between 0 to 5 Volt for a load of 7-200kg, see figure 2-5 for the scaling setup. The boom is mounted on a steel frame and a vertical step wise increasing load is applied. The reason why this strain gauges set is scaled to this range starting from 7 kg is that the strain gauge was not applied correctly and therefore starts with an offset. The strain gauges are applied under the green tape that can be seen in figure 2-5. The horizontal strain gauges are scaled with a resistance to give values between 0 to 5 Volt for a load ranging from 0-400kg, see figure 2-6. The steel frame is now rotated by 90 degrees so that the applied vertical load represents the horizontal load during sailing.

Calibration for the strain gauges is not important as the value is only a reference to later experimentally determine the applied force by the arm and the angle under which the forces

Figure 2-3: Experiment setup

are applied. Scaling of both the load cells and the strain gauges showed a linear behaviour between the force and the measured voltage difference. The relation between the applied load and the voltage is given in figure A-1, A-2, A-3 and A-4 in the Appendix.

The Arduino is programmed to read out the values of the sensors at a rate of 10Hz. A higher sample rate would lead to a too small time window to execute the experiment as the maximum

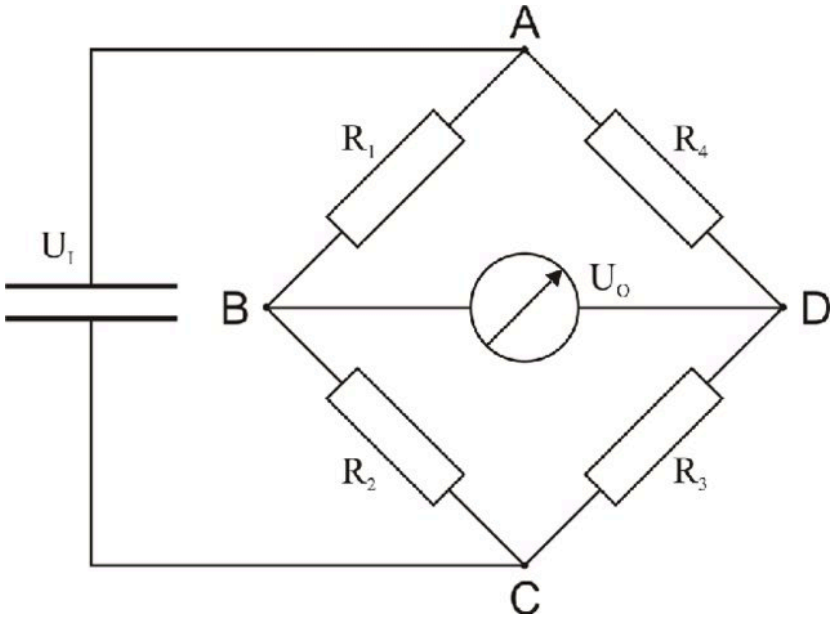

Figure 2-4: Wheatstone bridge

number of measurements is limited with this setup. A lower sample rate could lead to less accurate results as measurements with a too low sampling rate cannot represent an oscillating force.

2-3 Experiment results

2-3-1 Results of the water experiment

The experiment has been carried out in different sailing conditions to provide more insight in the loading on the boom under different conditions. The experiment has first been carried out in both flat water and small waves with winds between 16 to 22 knots with a 7.1 sqm sail and a medium wind board. The second experiment was in choppy water with winds between 24-32 knots with a 6.3 sqm sail and a high wind board. The results of the full experiment runs are given in the top of figure 2-7.

In this overview it can be seen that the experiments give reasonable results without excessive peak values for the two load cells and the horizontal strain. Unfortunately, the measurements of the vertical strain show some irregularities. This is probably due to a weak connection in the wiring of this sensor. Comparing the high wind experiment with the medium wind experiment it can be concluded that the loading on the boom is quite similar. From these experiments 20 time values and their respective measurements haven been chosen to further examine the loading on the boom. By choosing these 20 load cases a selection is made to have a wide range of load cases to be able to run the later FEM simulation for a wide range of load cases. All load cases have a recorded value of the vertical strain from the malfunctioning vertical strain gauges as this value is required to determine the angle of the loads. The load cases are given in table 2-1.

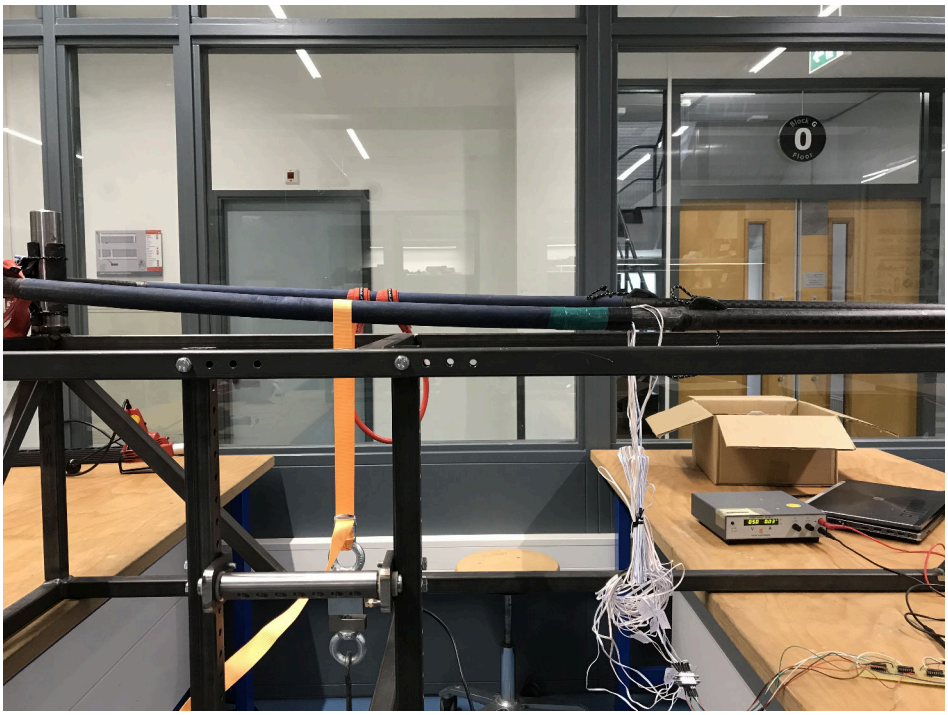

Figure 2-5: Scaling of the vertical strain gauges

Figure 2-6: Scaling of the horizontal strain gauges

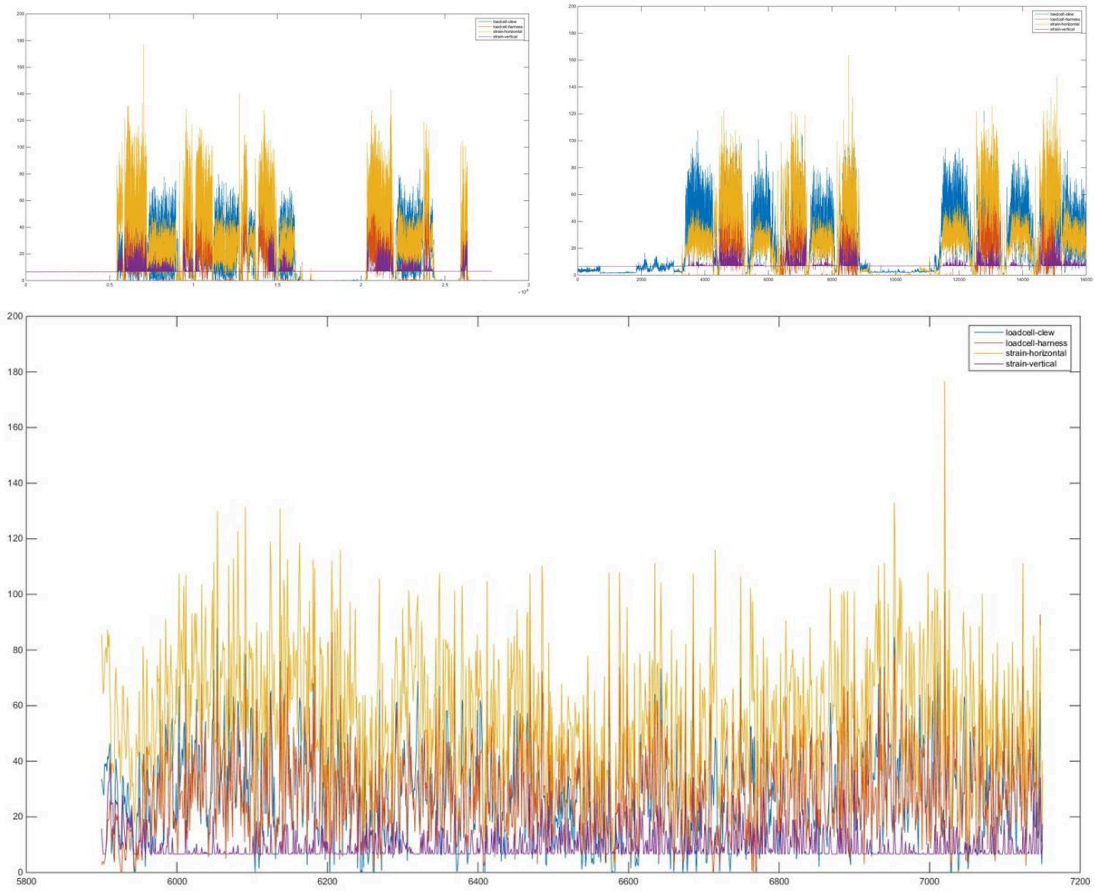

Figure 2-7: Experiment measurements

2-3-2 Determination of unknown force and angles

The boom is then mounted on the experiment setup and the loads on the load cells are then applied as can be seen in figure 2-8.

This loading on the boom gives values for the horizontal and vertical strain gauges. The loading by the arm of the rider is then simulated by applying an additional force with a force gauge until the strain gauges give the desired value. By doing this the loading by the arm of the rider can be found. The angles under which the forces are applied also determine the ratio between the horizontal and vertical strain. Therefore the angles are first estimated by looking at photos and videos of the rider, see figure 2-9. The angle is then further adjusted until all measurements are at the required value. The angle of the harness load can only be varied in steps of approximately 3 degrees. The angle of the force gauge can be adjusted in any orientation but the angle is given in steps of two degrees. The results of the 20 measurements are given in table 2-1. The loading by the riders arm appears to be more constant than the loading by the harness and the clew of the sail. This can be explained by the difference in stiffness between the force applying medium. The harness line and the clew of the sail are very stiff and therefore translate each small bump during sailing over waves and gusty winds into peak loading on the boom. In contrast, the arm of the rider is much more responsive and

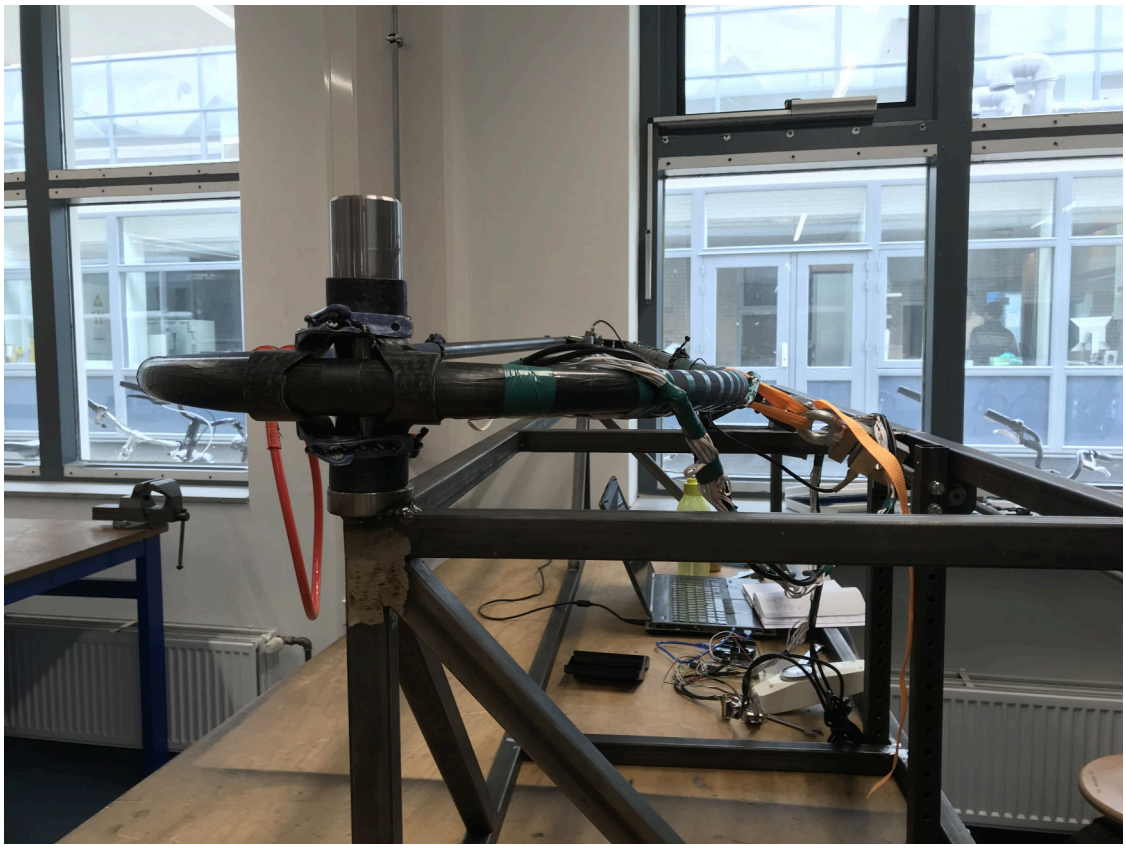

Figure 2-8: Experiment setup to determine the unknown load and angles

dampens out the bumps during sailing. The angle of the loads appears to be quite constant around 17-23 degrees for the harness load and 0-10 degrees for the arm load. This is also verified with an onboard Gopro camera where the change in angle of the loads is also analysed. A screenshot of this video is given in figure 2-9.

Figure 2-9: Screenshot of analysis video to visualize the change in loading angle

Table 2-1: Load cases with their loads and angles

Load Case	Clew Load [N]	Harness Load [N]	Angle [deg]	Arm Load [N]	Angle [deg]
1	368	362	17	130	8
2	497	510	17	132	4
3	554	433	23	130	10
4	488	427	20	138	8
5	743	556	20	172	4
6	695	497	17	180	2
7	704	888	17	168	0
8	1103	996	17	160	0
9	953	568	17	200	6
10	953	620	20	280	8
11	1025	673	17	142	2
12	548	248	20	228	6
13	659	408	17	204	4
14	608	482	17	124	4
15	194	165	17	132	0
16	711	694	17	142	8
17	461	539	17	138	2
18	369	491	17	108	2
19	1094	811	17	232	8
20	1226	810	23	281	10

Chapter 3

FEM fiber optimization

3-1 Introduction to Solidworks simulation software

This chapter will cover the work done with the Finite Element Method, FEM. A FEM analysis provides a cheap solution to perform an iterative design approach to optimize the layup. In this project the simulation software in SolidWorks is used to perform the FEM analysis. The SolidWorks software enables the user to define shells with a certain fiber layup which can easily be changed [15]. In the FEM analysis the carbon fiber material is represented with a custom orthotropic material. This means that the material properties differ per direction as described in section 1-2-1 and given in table 1-1. The setup menu for an orthotropic material in SolidWorks provides the user the ability to fill in all parameters and change them individually if necessary. The material properties that are used in the FEM simulation are given in table 1-1. These material properties are provided by the manufacturer for the unidirectional 6K fiber. These properties are also used for the biax fibers as the simulation software allows the user to specify the direction of the fibers with respect to the selected geometry. Therefore the material properties for a biax 6K fiber are the same as for the unidirectional fiber as the simulation software determines the stiffness of the entire model based on the orientation of the fibers.

In the simulation software the layup per section can be specified. The SolidWorks simulation software has a menu where the user can specify the layup per section with the number, thickness, orientation and material of the plies. The Solidworks interface is given in figure A-5 and A-6 in the Appendix. When the simulation is completed the mass of the part can be calculated based on the volume that is determined by the wall thickness per section.

The FEM model is scaled and validated with experiment results. After calibration the fiber layup is further analysed and then optimized for stiffness and weight.

3-2 FEM validation

3-2-1 Original layup and wall thickness

A FEM model is made from the existing Solidworks 3D files that were used to CNC the molds of the boom. The first step in the FEM analysis is to model the boom exactly like the boom that will be used in the experiments to validate the FEM model. This is done by sawing a boom with the same layup in multiple parts to be able to determine the wall thickness at each section of the boom. The sections with different wall thicknesses are shown in figure 3-1, where each color represent a section with a different wall thickness and layup.

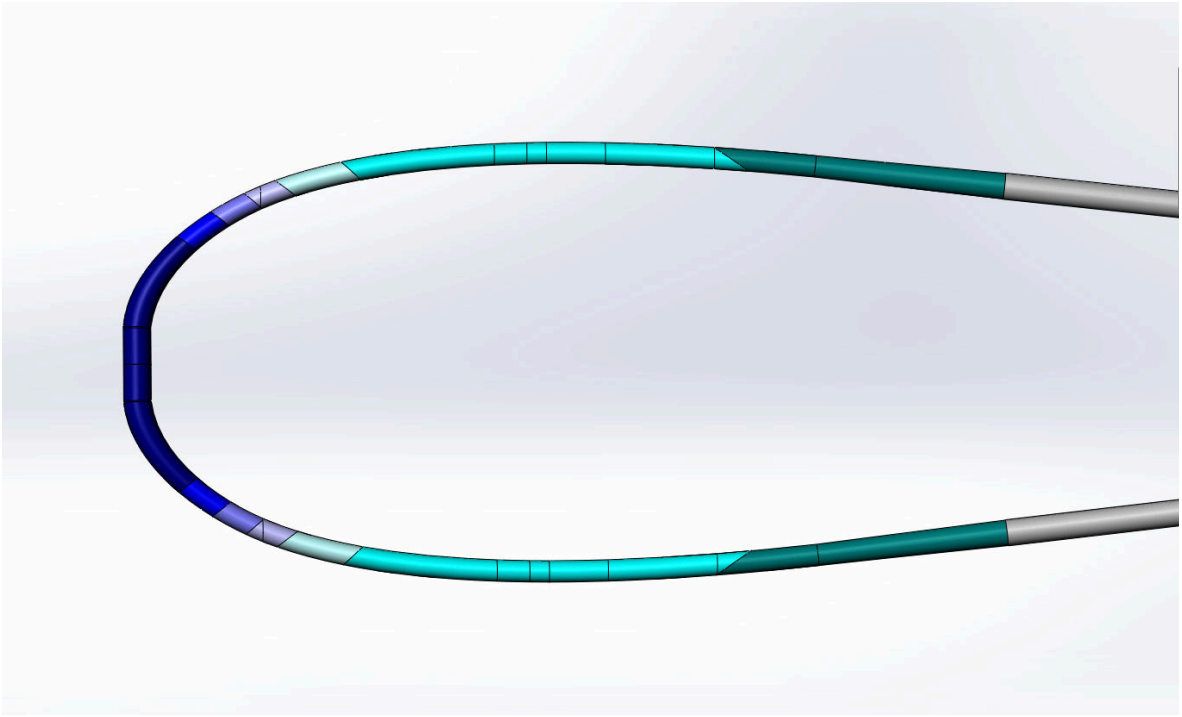

Figure 3-1: Boom sections with different layups.

As the layup consists of different fiber orientations the thickness per layer needs to be known. The thickness given by the manufacturer might not be representative as the thickness is influenced by the pressure applied during the curing of the resin. The thickness per layer is therefore determined by ratio of the weight of the fiber weave per square meter and the total thickness of the stack after curing. The different fibers and their thicknesses are given in table 3-1

The original fiber layup of this boom was determined by an iterative process where a few layups have been tested on the water. The layup is given in figure 3-2 and table 3-2. The layup is partly limited by the production process as described in section 1-2. Therefore the layup is divided in three sections; two sections starting at each end of the arms of the boom, and one section in the front of the boom. This limits the maximum curve in each section allowing the fibers in the plies to translate to the required position. The division in sections also lead to sections where the fibers from the front overlap with the fibers from the back.

Table 3-1: Thickness per fiber weave

Fiber weave	Symbolic representation	Thickness [mm]
Unidirectional 6K sleeve	$\underline{u}$	0.415
Braided biax 6K sleeve	$\underline{b}$	0.382
Braided biax 3K sleeve	b	0.22
Unidirectional 6K fiber	u	0.382
Unidirectional 3K fiber	$u^{\frac{1}{2}}$	0.191

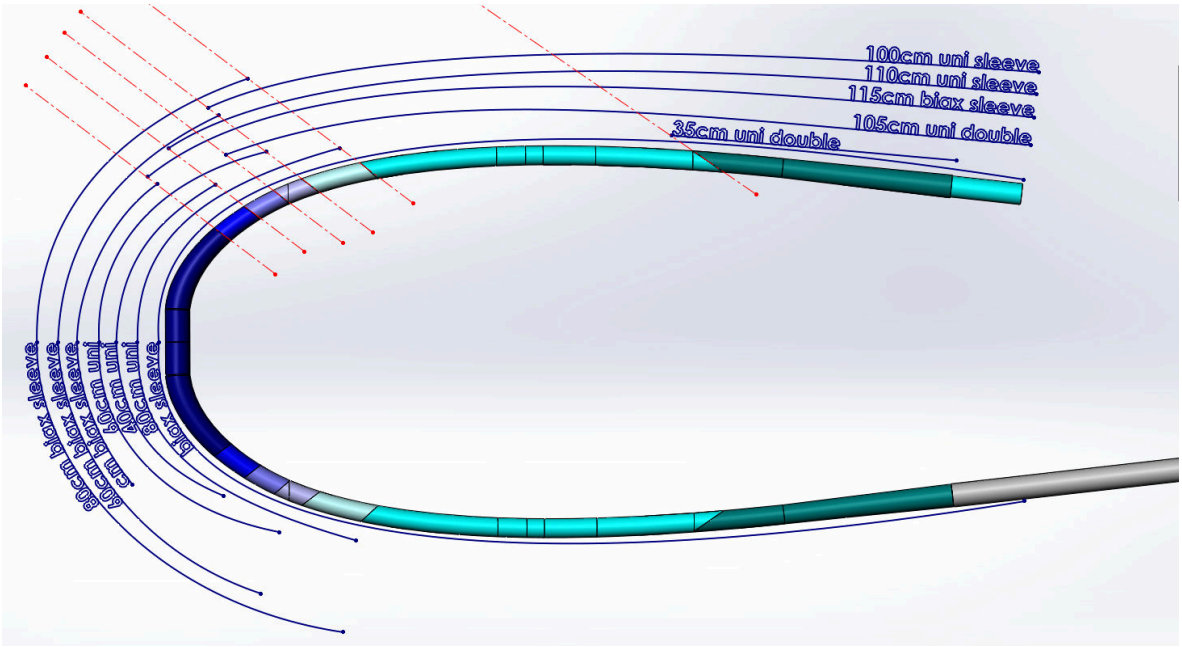

Figure 3-2: Schematic overview of the fiber layup

Each color in figure 3-1 represent a section with a certain wall thickness. The body of the boom is symmetric and does not only have the same wall thickness on each side of the boom but also over the diameter. The sections with their wall thickness and fiber layup are given in table 3-2. The colors in the table represent the sections with their respective color in figure 3-1. The fiber layup for each section is given in the last column of the table where for example $\underline{uub}uu\underline{b}$ stands for two layers of unidirectional 6K sleeve, one layer of biax 6K sleeve, two layers of unidirectional 6K fibers and one layer of biax 6K sleeve.

3-2-2 Validation experiment

To compare the FEM model to reality an experiment is carried out. In this experiment the boom is loaded with a step wise increasing load and the deformation is measured with a dial indicator with an accuracy of 0.01 mm. This experiment is done at two different locations on the boom. Two different load-deformation relations are needed to validate the FEM model. The FEM model will first be scaled with the load-deformation relation of the first location. After scaling with the first location the FEM can be validated with the load-deformation

Table 3-2: Wall thickness and fiber layup for different boom sections

Section	Wall thickness	Number of plies	Fiber layup
Dark blue	2.674	7	bbbuuub
Blue	3.091	8	ubbbuuub
Light Blue	3.471	9	ubbbuuuub
Purple Blue	3.122	8	uubbuuub
Grey Blue	2.358	6	uubuub
Purple Blue	3.122	8	uubuuuub

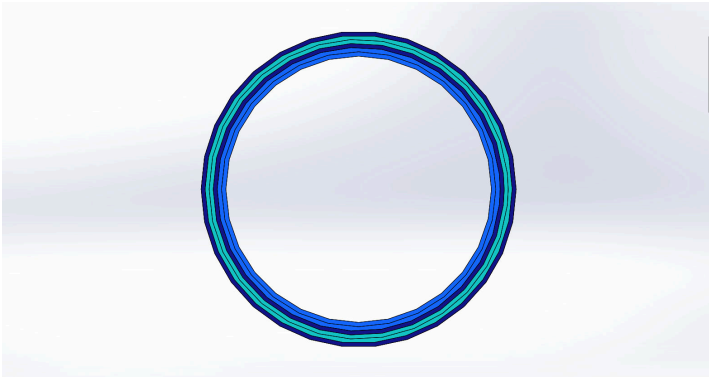

Figure 3-3: Boom cross section example

relation of the second location. For both experiments the deformation is measured at the point of maximum deflection. The two loading locations and the experiment setup are given in figure 3-4, where loading point one is given in red and loading point two in green.

The results of these experiments are plotted in figure 3-5. The load is step wise increase till 75 kg for location 1 and 70 kg for location 2. These maximum values are chosen as these are representable values of the loading on the boom during sailing as given in table 2-1.

From this figure it can be seen that the deformation shows a linear behaviour with respect to the applied load. For small loads the linear relation is not valid as can be seen in the figure. This non linear behaviour for small forces is probably due to the clearance between the two sliding tubes at the tail end of the boom. Once this clearance is gone and the load from the front section is also applied to the tail section the relation between the load and the deformation becomes linear.

3-2-3 FEM boundary conditions

The boundary conditions of the FEM simulation are modelled to represent the conditions of the experiment. The tail end of the boom is supported by a steel cylinder during the experiment to restrain motion in vertical direction, as can be seen in figure 3-4. This simple support is chosen for its simplicity in the evaluation of the results. Restraining the vertical translation at the tail gives the opportunity to measure the displacement of the boom without the need to account for the displacement of the support at the tail. Therefore the measurement taken with the dial indicator in figure 3-4 can be taken as the deflection of the boom. In the

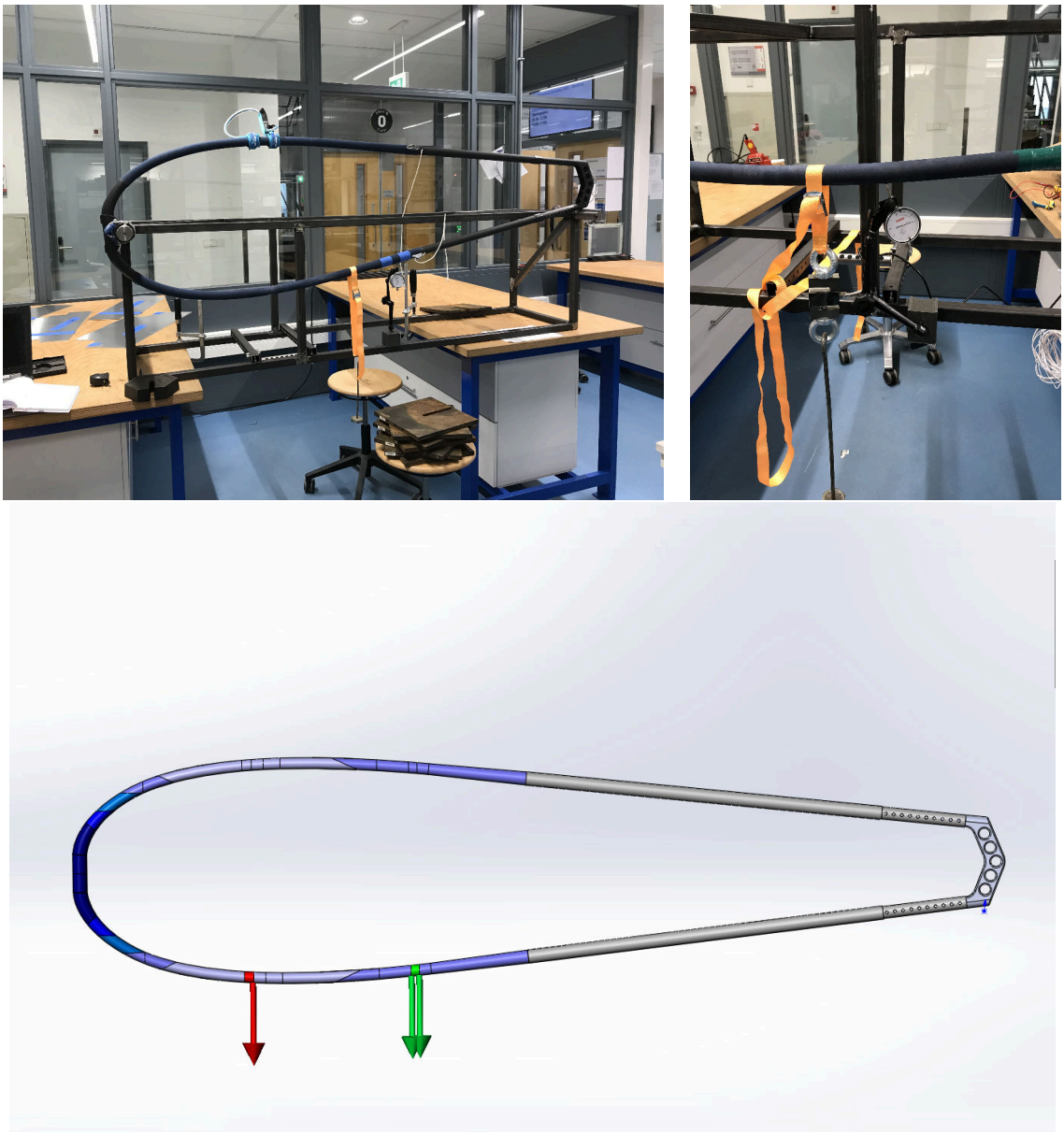

Figure 3-4: Experiment force-deformation relation

FEM simulation the same kind of support is modelled as can be seen in the right hand figure of figure 3-6. This support allows all motions except for the vertical translation. The front end of the boom is connected to the experiment setup with the boom head that is used during sailing. As the load in this experiment is vertical only the vertical restraint and the rotational restraint around the clamping area are considered. Both are assumed to be fully restrained. Therefore the support that is modelled in the FEM simulation is taken as a fixed geometry over the width of the boom head, given in the left hand figure of figure 3-6.

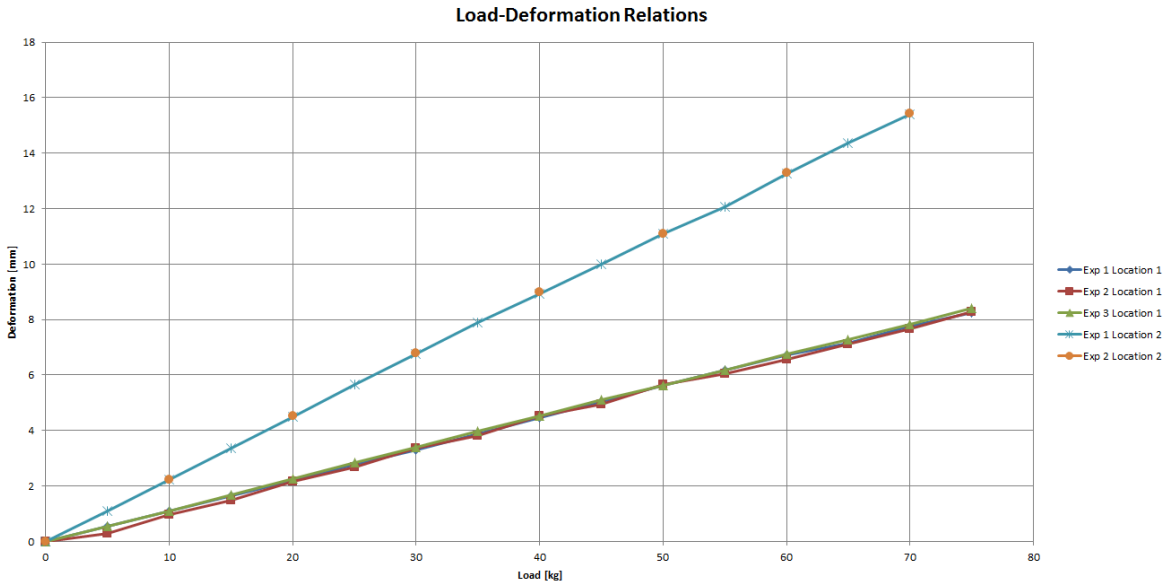

Figure 3-5: Load deformation relations for two locations.

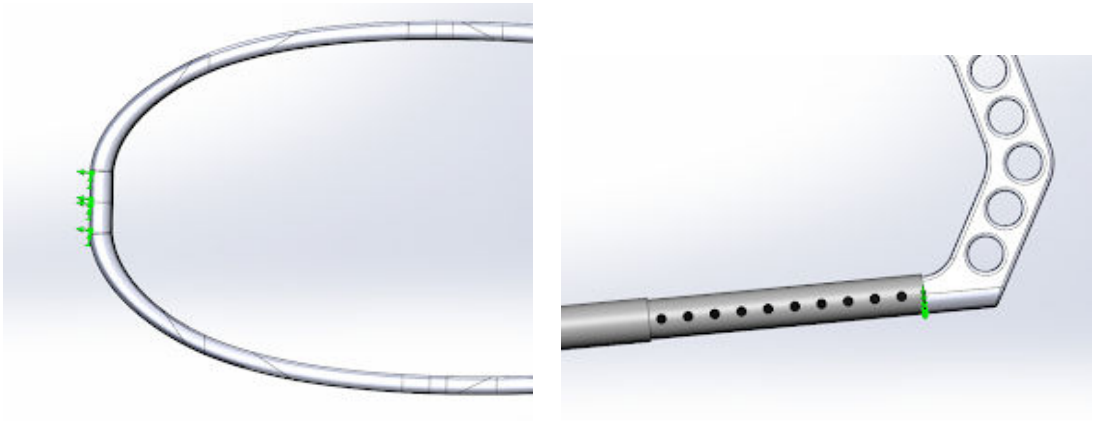

Figure 3-6: Boundary conditions FEM validation: supports

3-2-4 Scaling material parameters

Comparing the FEM model, modelled with material properties as provided by the manufacturer, with the experiment results shows that the FEM model predicts a stiffer boom than the given experiment results. The max deformation with the loading at point one is experimentally determined as 8.3mm where the FEM model predicts a deformation of 5.8mm. The FEM model is calculated with the material properties given by the manufacturer. These material properties are valid for a specific resin and curing requirements. Not all these requirements are met and therefore the material properties may not represent the material used in the boom. The material properties are for instance given for curing in an autoclave at 120 degrees, where this boom is cured with an outer mold with a vacuum and a pressurized tube on the inside at approximately 60 degrees. The material properties are therefore scaled to scale the FEM model to the experiment results at loading point 1. The straight tubes that

are glued to the body and the tubes of the tail end are not scaled as these pipes are made by industrial standards and should therefore meet the provided material properties. Scaling the material properties of the curved section of the boom with factor 0.78 calibrates the model with the experiment results of loading point 1. Applying the force at loading point 2 is used to control the reliability of the FEM model. The experimental determined deformation with the loading at point 2 is 15.4mm, the FEM model gives a deformation of 15.2mm. The validation results are plotted in the load deformation relations in figure 3-7. As can be seen the FEM model gives very small errors for the validation points compared with the experiment results for loading point 2. The error is between $1-2\%$ depending on the applied load. Therefore, is it assumed that the model is scaled correctly and can be used for further analysis of the fiber layup with reliable calculation results.

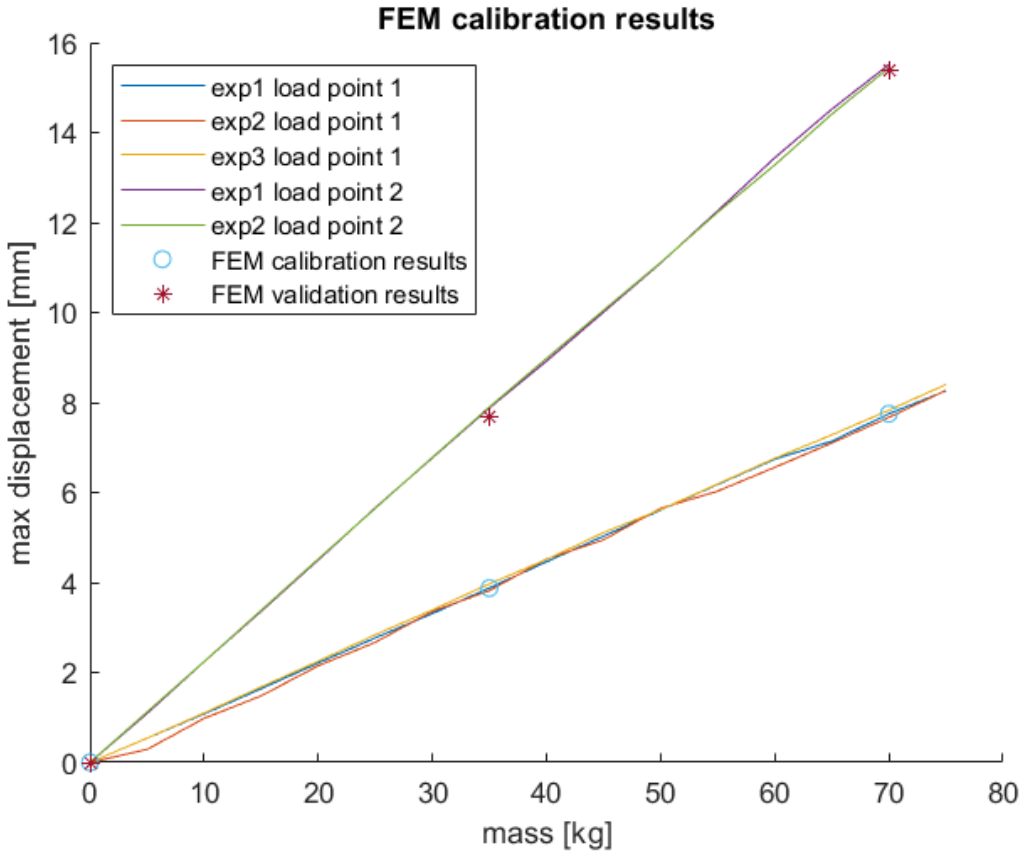

Figure 3-7: Load deformation relations with FEM validation points

3-3 FEM optimization

3-3-1 FEM optimization loading and boundary conditions

The FEM optimization simulations are done for two load cases given in table 3-3. Load case 1 is a load case determined from the load identification results given in table 2-1. In this

load case the boom is under full loading, meaning a high force on the harness line under a prescribed angle, a high load on the tail end of the boom and a smaller load exerted by the arm of the rider under a prescribed angle. The magnitudes of the loads and their angles are given in table 3-3. The second load case is a more simple load case that is used to get inside in the changes in stiffness per change in layup. This load case is chosen as there is only one force applied so the physics of the model should be easier to understand. Only the original layup is evaluated for more load cases to check the model for peak stresses and their location. It was concluded that the peak stresses under the load cases given in table 2-1 are much lower than the critical stress. Therefore it was decided to do the optimization with one representative full load load case and one simplified load case.

Table 3-3: FEM load cases with their loads and angles

Load Case	Clew Load [N]	Harness Load [N]	Angle [deg]	Arm Load [N]	Angle [deg]
1	711	694	17	142	8
2	0	0	0	700	0

Load case 1 represents the loads exerted on the boom during sailing. Therefore the boundary conditions to the simulation should be modelled accordingly. During sailing the boom is attached to the mast with a boom head. The forces exerted on the boom by the sail and the rider and the reaction forces on the boom head keep the boom in position. The model is restrained at two locations, the front end of the boom at the boom head and at the tail end. The boom head is a carbon part that transfers the loads from the boom to the mast. The sections that carry the load are made of 3-4mm solid carbon making the boom head a very stiff part. Therefore it is assumed that the deformation of the boom head will be much smaller then the deformation of the boom. In reality the deformation of the boom head will allow for some very small rotations as all translations are fully restrained by the boom head. The small rotations due to deformation of the boom head are neglected, therefore the support in the FEM simulation is modelled as a fixed geometry over the width of the boom head, restraining all translations and rotations. This assumption will lead to a small difference in displacement of the boom sections with respect to a stationary point. However, during the optimization all layups are tested with the same boundary conditions. The change in performance in stiffness of the curved section itself due to the different boundary condition at the front section is assumed to be very small. Therefore this small error is accepted and the model is simplified with the fixed boundary condition. The boom head connection and the FEM fixed geometry representation are given in figure 3-8.

The tail end support is modelled at the center of the tail to restrain translations in vertical and horizontal direction, translation of the tail end in direction of the in plane and out of plane components of the harness line force is therefore restrained. The support does allow for all three rotations and translation in horizontal direction, which is the shortening of the boom in direction of the clew load. The support and its location are given in figure 3-9. In reality the tail end is connected to the sail with a rope and pulley system. The tail end of the boom is kept in place as the applied loads on the rig are in equilibrium. Choosing these boundary conditions simplifies the model while still being representative.

Figure 3-8: Boundary conditions FEM optimization: Boom head

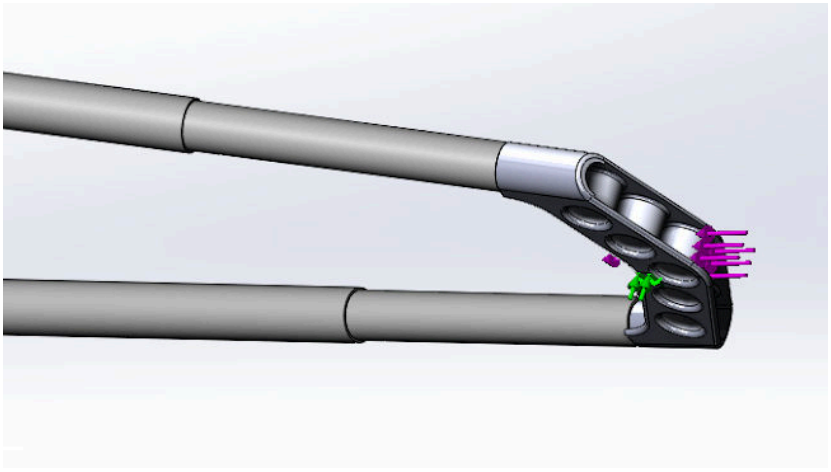

Figure 3-9: Boundary conditions FEM optimization: Tail end

3-3-2 Creation of new layups

The optimization of the fiber layup is then carried out as an iterative systematic process where the layup per section is changed and the difference in stiffness and weight is evaluated. The change in layup per section is based on the stress and displacement results of the previous iteration and/or basic engineering intuition. In the stress results of the simulation the maximum stress in each ply can be found at any location. This is mainly used to optimize the biax plies and their thickness per section. Initially, during this process the layup of the fibers is slightly simplified by neglecting the overlap from the fibers that are laid from the front section and from the back section. Based on the stress distribution of the original layup the boom is divided in different segments to vary in fiber layup over the location on the boom. The boom with its segments is given in figure 3-10.

Based on the original layup and its stress distribution the fiber layup per section is altered and the changes in stress, deformation and mass are saved. This iterative process is done for each section to give an insight where a reinforcement in the layup gives the highest increase in stress and deformation reduction with the lowest increase in mass.

The simulation results are saved for the max displacement and tail displacement for load case 1 and for the horizontal displacement for load case 2. An example of the simulation results can be found in figure 3-11.

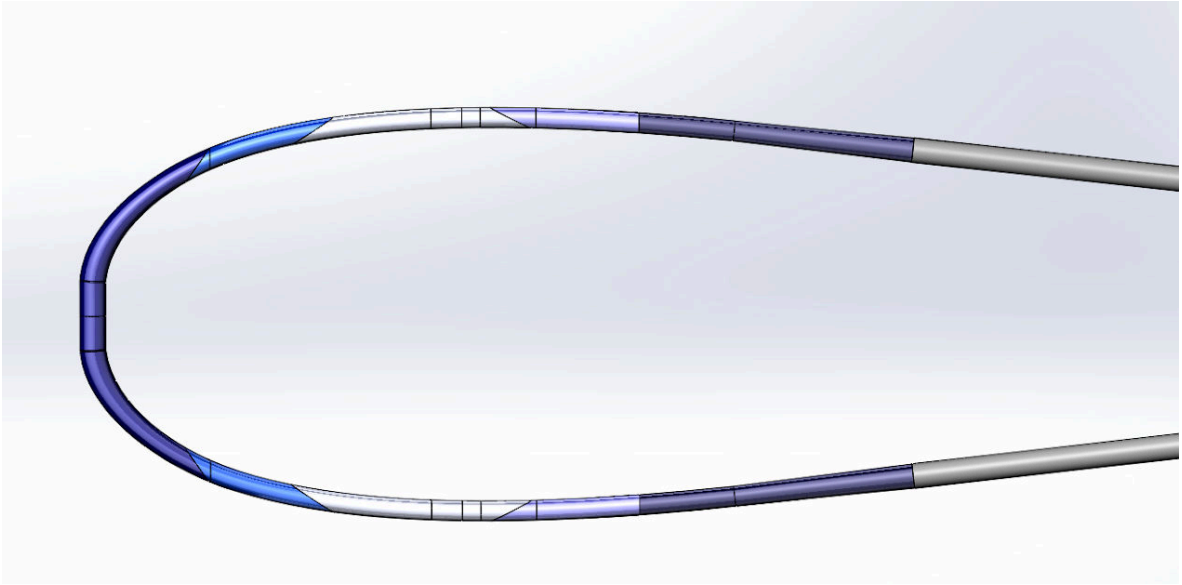

Figure 3-10: Boom divided in segments

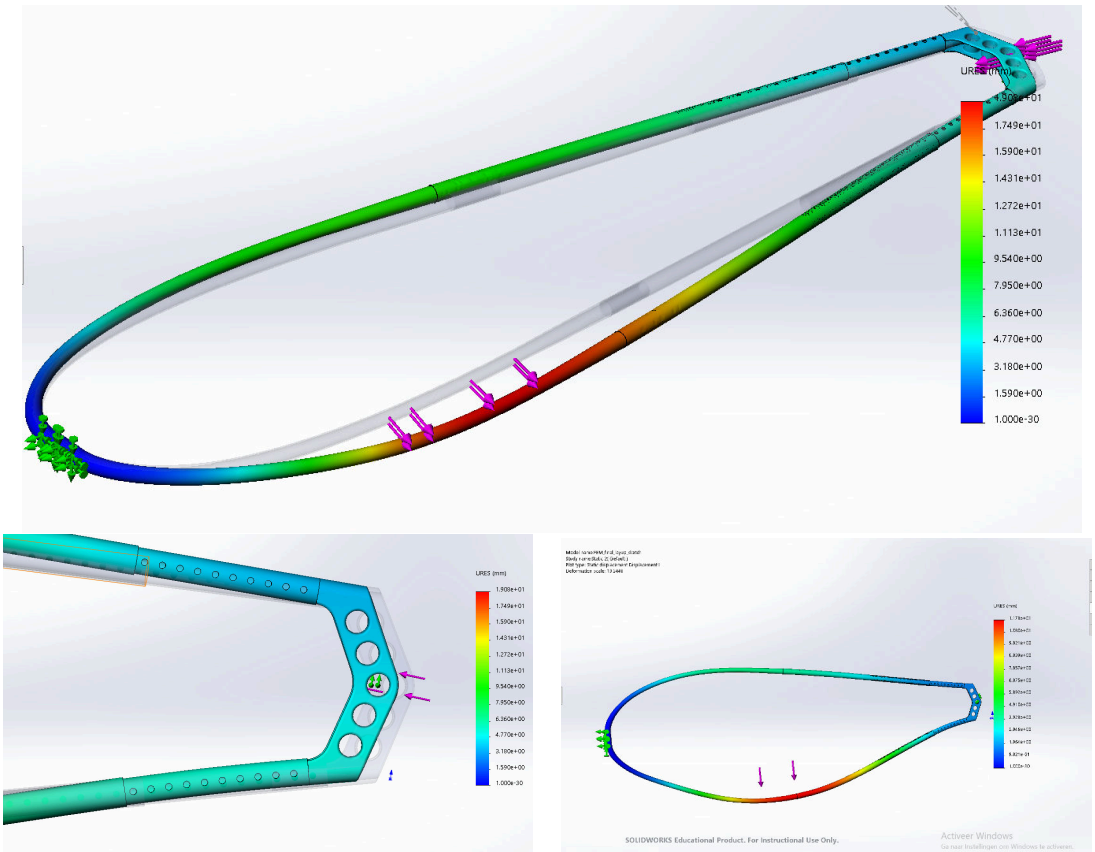

Figure 3-11: Simulation results for the different load cases

In total 50 iterations with different fiber layups have been made. The first iterations were

merely done to give insight in the change of stiffness vs mass for each section. Later iterations were performed to find a final layup where the best layup of each section was chosen. The results of displacement vs mass are given in figure 3-12. The top figure of figure 3-12 gives the relation between the mass of the layup and the max displacement under load case 1 as described in table 3-3. The left hand figure in figure 3-12 gives the relation for mass and tail displacement under load case 1. The right hand figure of figure 3-12 gives the relation between mass and horizontal displacement under load case 2. The layup data is also given in table A-1 in the Appendix.

The original layup is encircled in red as a reference for the results. The red vertical line in the plot is a selection line for the maximum mass that is allowed for this part of the boom. This selection line represents a limit of a $100g$ mass increase to ensure a significant mass benefit over the competing market. All layups on the right hand side of this selection line are therefore discarded as they are too heavy.

3-3-3 New layup selection

To find the best performing layup for both stiffness and mass the results are evaluated with the performance equation 3-1.

$$\gamma = \frac{1}{\alpha * \delta + \beta * m} \tag{3-1}$$

This equation is used to express the performance in both mass and displacement in a number. This number needs to be maximized for the best combined performance. With the coefficients α and β the weight of the two variables, mass and displacement, is determined. The coefficients are chosen so that both variables have equal weight. β is taken as 1, α is for each case determined with equation 3-2.

$$\alpha = \frac{m}{avg(displacement)} \tag{3-2}$$

The performance of each layup for maximum displacement under full loading, load case 1, is given in the top figure of figure 3-1, for tail displacement under full loading in the left hand figure of figure 3-1 and for horizontal displacement under a horizontal load, load case 2, in the right hand figure of figure 3-1.

In this figure the highest positioned star gives the highest performance. In all figures the best result is obtained for the layup given with a blue star, named base layup in the legend. This layup has been chosen to further evaluate. After some iterations the layup represented with the cyan star was found. This layup is still based on the division in sections as shown in figure 3-10. The next iterations where done to further optimize the length and location of the sections. The black and purple stars represent two identical layups with different section length and location. Based on the performance equation the layup presented with a black star has been chosen as the new layup. The circle in the plot representing the final layup is the black star layup including the necessary overlap of fibers coming from the front and back sections of the boom. This leads to an increase in weight and only a very small increase in stiffness. This leads to a position in the plot that represents a weaker performance based on the performance equation 3-1. More about the overlap section can be found in section 3-4-1.

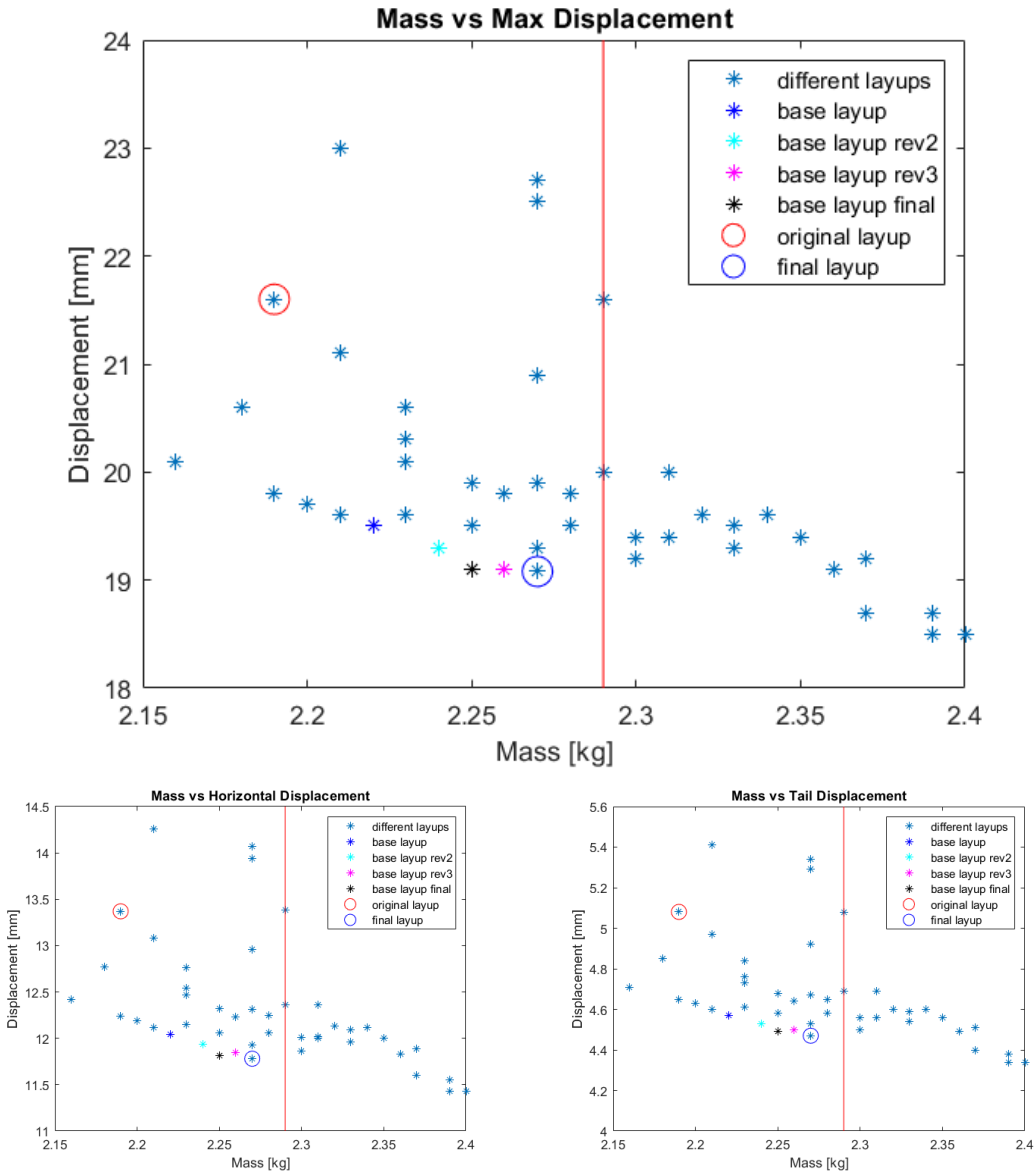

Figure 3-12: Mass-displacement relations for different fiber layups

3-4 Final Layup

The final layup is given in figure 3-14.

The layup per section is given in table 3-4.

3-4-1 Fiber overlap

The purple section in figure 3-14 is the section where the fibers overlap. The overlap of fibers is needed because the unidirectional fibers cannot follow the full curve of the boom as described in section 1-2-3. Therefore the best option for the overlap of the fibers has been

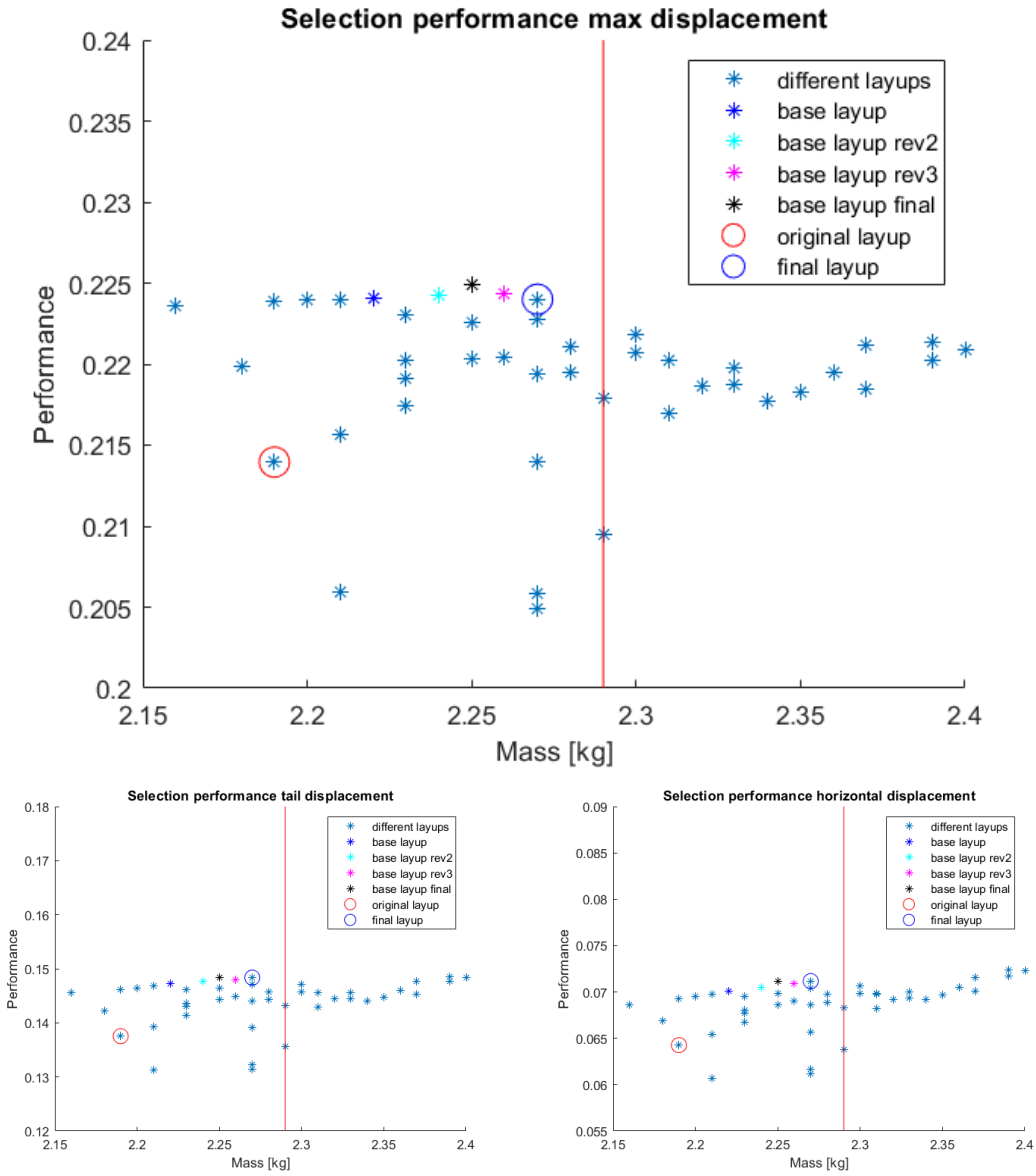

Figure 3-13: Weighted performance of different layups

Table 3-4: Wall thickness and fiber layup for different boom sections

Section	Wall thickness	Number of plies	Fiber layup
Dark blue	3.276	9	$\underline{\text{bbbu}}^{5}\underline{b}$
Purple	3.691	10	$\underline{\text{bbbuuu}}^{4}\underline{b}$
Blue	2.947	8	$\underline{\text{ubbbu}}^{3}\underline{b}$
Grey	2.215	6	$\underline{\text{buuuub}}$
Light Blue	2.401	6.5	$\underline{\text{buuu}}^{2.5}\underline{b}$
Purple Blue	3.533	8.5	$\underline{\text{buuu}}^{4.5}\underline{b}$

layup.png

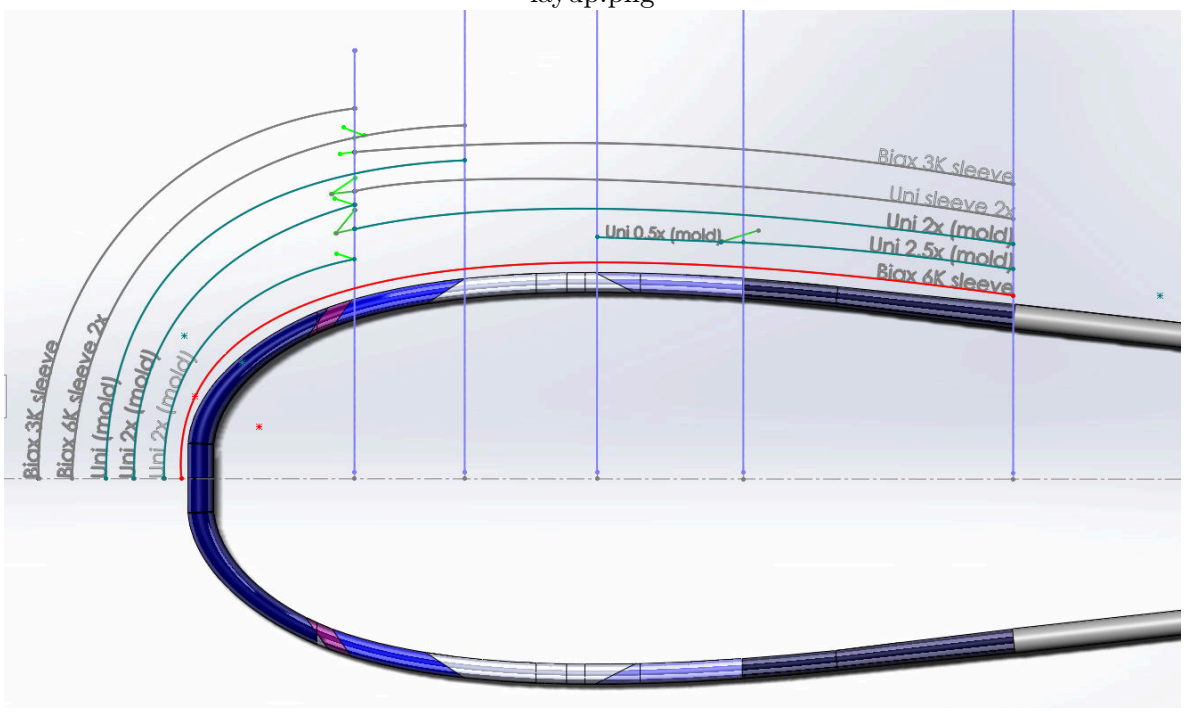

Figure 3-14: Schematic overview of the final layup

investigated. The overlap of the fibers is important as the overlap section is close to the highest stress section. Therefore the overlap section should be able to transfer the stress from fibers coming from the front to fibers from the back while also the mass objective needs to be satisfied. Based on the literature study the length of the overlap section is chosen as 40mm [16][17]. This overlap length ensures an overlap section that is stiffer than the other sections but sacrifices the fatigue life to some extent. A schematic overview of the fiber overlap can be found in figure 3-15. The colors represent the colored sections of the boom as given in figure 3-14. The first three unidirectional layers, after the red biax layer, have a overlap that is alternating [16]. The dashed purple lines show the required length of the fiber. The fiber should end somewhere in the dashed purple line. If the fiber ends before the dashed line a weak spot is formed as this leads to a smaller wall thickness in that area. The fibers that are continuous in this schematic figure, two times biax 6K and one unidirectional fiber, are coming from the dark blue front section and will end in the blue section and are therefore able to make this curve.

3-4-2 Main differences with original layup

Table 3-5 gives an overview of the main differences and their influence on the stiffness and mass of the boom. From this table it can be concluded where it makes most sense to add mass to reduce the displacement. Adding one layer of unidirectional fibers (UD) in the dark blue and the purple blue sections give the highest ratio of displacement over added mass and are therefore the sections that should be reinforced to obtain the project goal.

The new layup differs from the original layup as can be seen in table 3-5, or by comparing

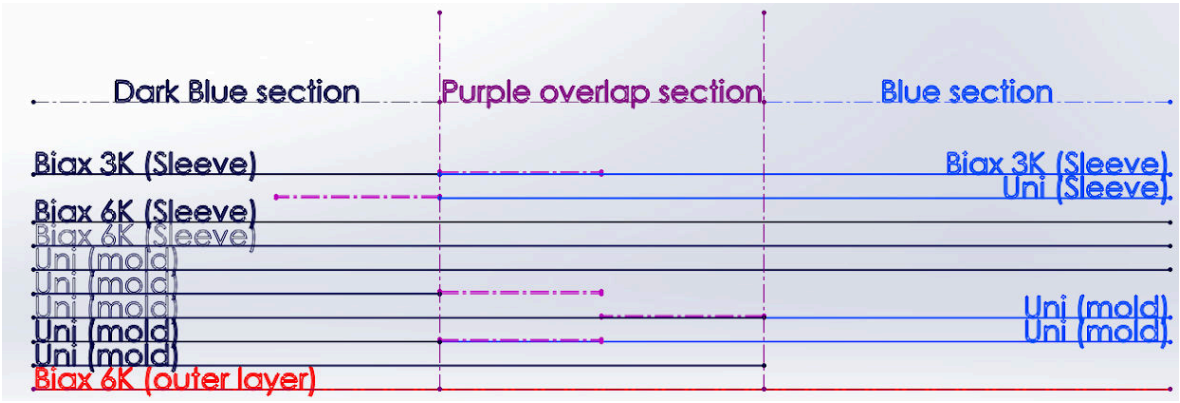

Figure 3-15: Schematic overview of fiber overlap

Table 3-5: Main changes and conclusions in layup and their differences for displacement and mass

Layup	section	displacement [mm]	mass [kg]
Original layup	all	13.38	2.19
New layup	all	11.78 (-1.60)	2.27 (+0.08)
Change inner biax to 3K	all	+0.36	-0.09
Change order to biax first	all	-0.42	0.00
Add 1 6K UD	Dark blue	-0.23	+0.04
Add 1 6K UD	Blue	-0.14	+0.03
Add 1 6K UD	Purple blue	-0.39	+0.06
Add 1 3K UD	Light blue	-0.11	+0.02
Optimization of section length	all	-0.32	+0.02
bbb inner biax optimal	Dark blue, Blue		
b inner biax optimal	Grey, Light blue, Purple blue		
b outer biax optimal	all		

figure 3-2 and table 3-2 with figure 3-14 and table 3-4. First of all the inner layer of the boom is now made of a 3K bi-axial fiber sleeve, compared to 6K bi-axial sleeve that is used as third layer in the back and first layer in the front. Moving this layer to the inside of the circular cross section allows the unidirectional fibers to move to the outside of the circular cross section. Moving these fibers to the outside increases the stiffness as the moment of inertia increases to the power of four. Given that the E-modulus in the main stress direction is much higher for the unidirectional fibers, as these fibers more or less align with the main stress, the stiffness increases significantly. The mass is also reduced by using the 3K sleeve instead of the 6K sleeve, as the 3K sleeve is thinner. This is the main reason that the new layup can use more layers of unidirectional fiber in the reinforcement sections without adding too much mass. The main difference in stiffness is achieved in the front section. The new layup has more unidirectional fibers in the dark blue section. This section is also extended so that the larger wall thickness is being used over a larger length. The next section, the purple section, that has the overlapping fibers is also different. Where in the original layup the overlap is done in multiple sections over a longer length the new layup has only one short overlap section. The blue section has a smaller wall thickness than the original layup due to

the change in overlap section, the grey section has the same layup but the location and length of the section has been changed. The second main difference is made in the purple blue and light blue sections. These extended sections have an additional layer of unidirectional fiber making the boom stiffer with a small added mass. The extension of this section has proven to be very important.

Chapter 4

Results

To evaluate the new layup and basically the entire project two booms with the new layup have been made. The two booms both have the same final layup as given in figure 3-14. Two booms have been made to compare the results between the two booms and to exclude eventual invalid results.

4-1 Determination of final layup performance

The two booms have been evaluated with the same experiment as described in section 3-2-2. For this evaluation the boom with the original layup has been measured again as well. The boom is mounted to the steel frame with the boom head at the front section and supported at the tail end by the frame. The boom with the original layup and the two booms with the final layup are mounted with the same boom head and tail end to exclude differences due to these factors. The boom is loaded at the two loading points as given in figure 3-7 while the deformation is measured at the point of maximum deflection with a dial indicator as given in figure 2-3. The displacement of the boom per location is predicted with the FEM model for a step-wise increase in load up to 70 kg. The real load deformation relation is determined with the experiment to evaluate the performance of the new layup. The results of the FEM data versus the measured data is given in figure 4-1.

As given in figure 4-1, the displacement at the point of maximum deflection for loading at point 1 is predicted with a high accuracy. The error for the measurement versus the prediction is 2-4 percent. Where the two new booms give very similar values with a deviation of less than 2 percent. With these results it can be concluded that for a loading at the location of the harness lines, where the main loading is applied, the new layup is approximately 16 percent stiffer than the original layup. Furthermore, it can be concluded that the results of the FEM simulation for this location are accurate. However, the results for the second loading point show that the new layup is only 5.5-7.5 percent stiffer, while a 13 percent increase in stiffness was predicted by the FEM simulation. As both booms with the new layup gave the same result a fabrication fault is not very likely. The original layup is only measured for one boom,

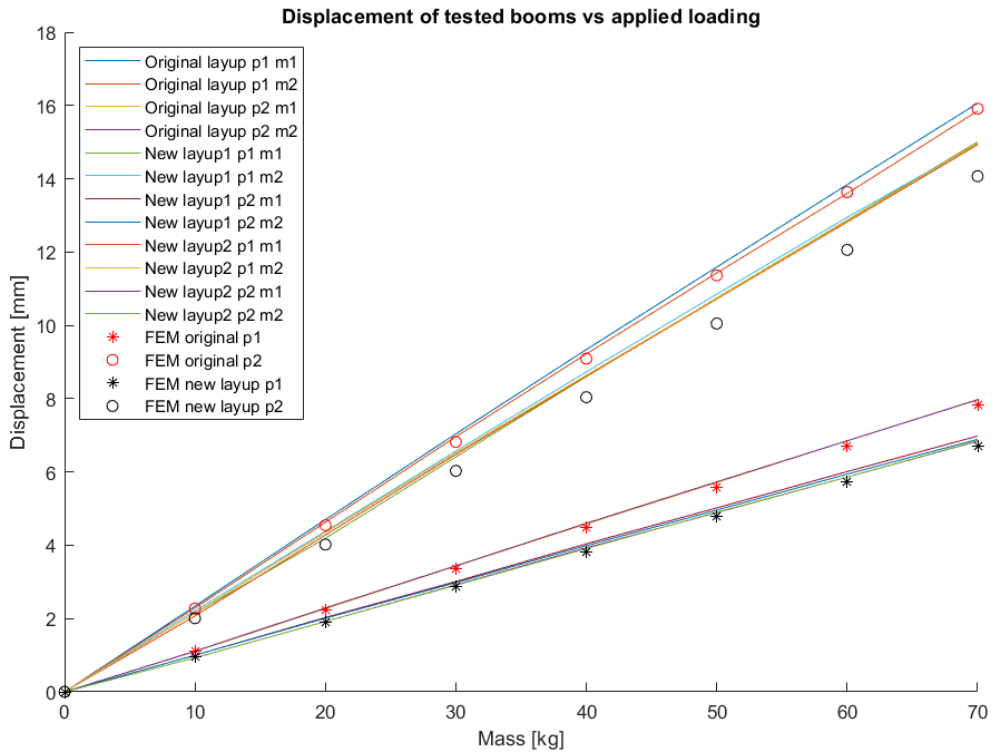

Figure 4-1: FEM prediction of displacement per location vs measurements for the original vs the new layup

but as it was measured at both arms of the boom with equal results a different behaviour, with respect to other booms with this layup, is also not very likely. As all tests are performed with the same tail end and boom head the only difference per boom is the optimized front section and the industrial fabricated tubes that are glued to the front section. The boom with the original layup is made with tubes that are manufactured in Croatia, the new booms are made with tubes that are manufactured in China. Both tubes are ordered with the same specifications. However, it is very likely that a part of the change in measured displacement and predicted displacement is due to these tubes. The FEM simulation shows that if the E-modulus of the material of the tubes is changed that the displacement due to loading at loading point 2 will become significantly larger, where the displacement due to loading at loading point 1 barely changes. Reducing the stiffness with 10 percent make the FEM results converge closely to the experiment results. As the FEM model is validated and scaled with the tubes that are manufactured in Croatia the difference in prediction vs experiment results can be due to these tubes.

4-2 Evaluation of final experiment results

The experiment results have been evaluated with the performance equation 3-1. As the experiment results differ from the simulation results it is possible that the old layup has a

better performance based on this equation as the difference in displacement is small but the new layup is heavier. The results are given in figure 4-2. This figure shows that for loading point 1 the new layup is much better as the performance number should me maximized. The performance number of the new layup is 6 percent higher than for the original layup. However, for loading point 2 the difference in performance between the two layups is much smaller, the new layup scores 1.3 percent higher. The new layup is still favorable as the performance number is higher.

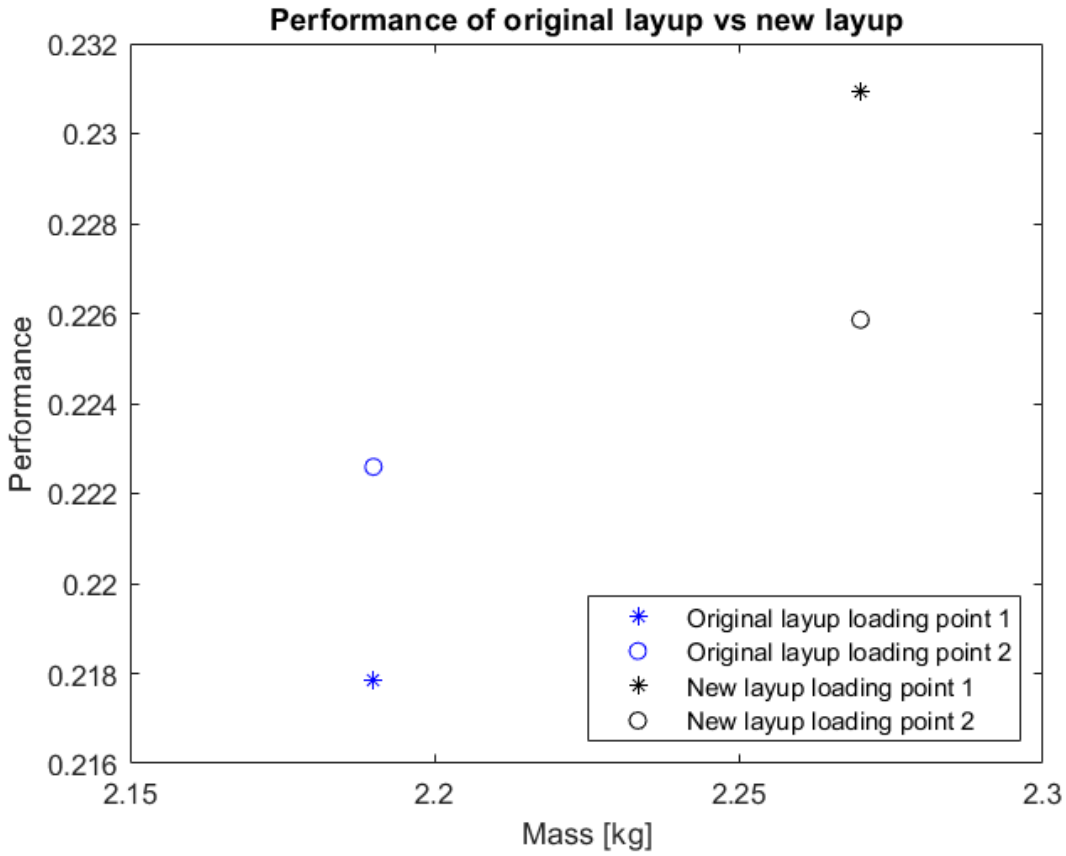

Figure 4-2: Performance comparison between the original layup and the new layup based on the performance equation.

4-3 Evaluation of new layup during surfing

The new booms are also evaluated during a windsurf session on the water. The test is done by the author, Pieter Bijl the co-founder of the Proboom project and one other non biased surfer, Wouter.All three surfers have more or less equal surfing skills. The test is performed by lining up and evaluate the difference in speed where each surfer is using a different boom, see figure 4-3. During the first test session one of the surfers is using the same boom during the entire test session while the other two change booms to determine the difference in performance. This cycle is repeated two times so that all surfers tried all booms to be able to compare

the booms and their performance. As base reference the third boom was a Neilpryde X9 boom, by many regarded as the best boom on the market. The difference in performance is difficult to quantify as the surfer skills, wind and water conditions determine most of the difference. However the personal feeling after the test sessions is easier to describe and discuss. From this test it was concluded by all three surfers that the new layup is an enormous step forward compared to the Neilpryde X9 boom and the original layup. The 16 percent increase in stiffness in the front section makes a big difference as this makes it easier to power and depower the sail, but also to adjust the pressure via the boom through the mast on the board. This is used to prevent the board from flying too much during stronger gusts. The small increase in stiffness seen at the second loading point does not feel as such a small difference as the main loading is applied closer to the first loading point.

Figure 4-3: Lining up with Wouter to compare the performance of two different booms.

Chapter 5

Conclusions

This chapter gives an overview of the project and its main conclusions and recommendations.

The loads on the boom during sailing are determined with an 'water' experiment and an onshore experiment. For the water experiment a boom is equipped with a load cell for the harness load and a load cell for the clew load. The total loading is captured with two sets of strain gauges. The sampling rate of the processing Arduino was set to 10Hz. The experiment results, shown in figure 2-7, do not show a perfectly fluent curve for the loads, meaning a higher sample rate would be required. However, due to the limitations of the Arduino combined with the experiment setup a higher sample rate could not be implemented as this would reduce the maximum testing time too drastically. Looking at the results it was concluded that the too small sampling rate did not lead to invalid results. This was concluded based on the peak values of the entire experiment time run. There were no excessive peak values recorded meaning that the recorded values are values that happen frequently, and therefore represent the peak loads during sailing. Combining the water experiment with the onshore experiment the loads and their angles were known. The angle of the harness load was determined based on the values of the horizontal and vertical strain gauges. The angle was determined with a step size of approximately 3 degrees as this was the smallest step on the experiment setup. The angle of the arm load of the rider was determined with a step size of 2 degrees. The step size in angles are quite large, however the difference in angles between the load cases appeared to be very small. This was validated with an onboard Gopro camera where the angle of the loads is visible. With these experiment results 20 load cases were introduced. None of the 20 load cases led to critical stresses in the boom and therefore one of the average high load cases was chosen to use for the FEM optimization. This load case was chosen as a too high load case might have led to an over designed boom and a too low load case gives a much smaller difference in displacements making the distinction between the layups more difficult. This load case was also chosen as the ration between the harness, clew and arm load was representative for the average high load load cases.

During the optimization the displacement under loading and the mass of the layup were saved and plotted in figure 3-12. The final selection of the new layup was done based on a performance equation, given in equation 3-1. The coefficients are determined so that the two

parameters, mass and displacement, have an equal weight. This does not necessarily mean that a different surfer will decide that this is the best layup, as a different surfer may value weight over stiffness or the other way around. This means that the coefficients might differ for different surfers based on their personal preferences. Changing the coefficients may lead to a different optimal layup. Figure 5-1 shows the performance of the generated layups for different weight factors. From this figure it can be concluded that for coefficients where the stiffness is the leading criteria the chosen layup performs best. If the mass is the leading criteria with a weight factor of 2 over the stiffness the chosen layup is no longer the favorable layup. However the difference between the best performing layup and the chosen layup is very small.

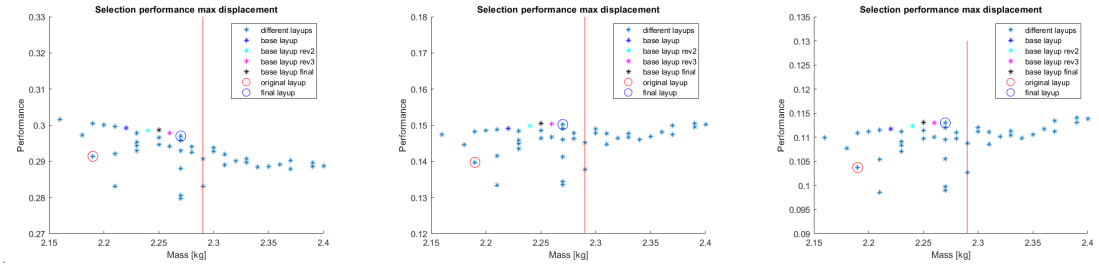

Figure 5-1: Weighted performance for weight factors $0.5\alpha, 2\alpha, 3\alpha$

The layups in figure 3-12 are simplified, meaning that there is no fiber overlap zone implemented. A fiber overlap zone barely influences the stiffness but does add a certain amount of mass. The chosen layup is therefore updated in figure 3-12 with the added overlap zone. This overlap zone is designed as 40 mm long, with an alternating overlap leading to an added mass of 0.02kg. The original layup had multiple longer overlap sections and therefore a larger added mass. The original layup without these overlap sections would therefore occupy a higher spot in the performance figure.

As given and discussed in section 4 the results of the final experiment show that this project resulted in a new layup that is significant stiffer for a small increase in mass. For loading point 1 the FEM prediction was accurate and the new layup proved to be 16 percent stiffer. For loading point 2 the FEM predicted stiffness was not reached during the experiment. The FEM simulation predicted that the new layup was 13 percent stiffer than the original layup. The results showed that the new layup was only 5.5-7.5 percent stiffer than the original layup. Section 4 describes the possible difference due to a change in manufacturer for the tubes that are glued to the body of the boom. The FEM simulation was recalculated to determine whether a small change in stiffness of these tubes would lead to different displacement results under loading at loading point 2. The FEM simulation showed that for a 10 percent decrease in Young's Modulus the FEM simulation results converged closely to the experiment results.

The project goal was stated as: Optimize the fiber layup for a light weight and stiff carbon windsurfing boom. The new layup was selected based on the performance equation 3-1, with the coefficients chosen so that both mass and displacement have equal weight. The experiment results of both the new layup and the original layup were evaluated by the same performance equation. Based on these results, given in section 4-2, it can be concluded that the new layup is better for both loading points and therefore optimized for weight and stiffness compared to the original layup. The project goal is therefore achieved. The boundary condition that the boom should not fail under normal loading is also reached. The FEM showed that in order

to achieve optimal performance the boom is so stiff that the peak stress is much lower than the critical stress. Increasing the stiffness compared to the original layup led to even lower stresses.

For the layup of the boom a sandwiched layup of unidirectional fibers with biaxial fibers at the inside and outside of the circular cross section was determined as the best performing layup for the sections loaded under bending. For sections that are loaded under both torsion and bending additional layers of biaxial fibers are added at the inside of the circular cross section. These biax fibers are added at the inside as the unidirectional fibers are used at the outside to create the largest moment of inertia for these fibers as the displacement due to bending is leading in this case. Even the small translation of the unidirectional fibers from the inside to the outside of the layup makes a significant difference. This conclusion can also be used for general slender carbon tubes.

Based on this project it can be concluded that the windsurfing industry, and maybe more small sport industries, could use a more scientific approach to their product designs. This conclusion is based on the fact that the original boom, which is seen by many professional windsurfers as one of the best booms on the market, has been optimized with an average increase of stiffness of 11 percent. The water evaluation showed that the new layup felt much better than the Neilpryde X9, which is seen as one of the best booms on the market. However, this water evaluation is partly based on personal preferences.

Future work to complete the optimization of this boom might be the optimization of the tail end of the boom. The tail end of the boom is, like the Dark blue and Blue section of the boom, a section where the stress reaches its maximum values. The weight of the tail end is already very low but the weight is located at the end of the boom influencing the swing weight significantly. Therefore a small decrease in mass might increase the feeling of the boom even more. The stiffness of the tail end influences the overall stiffness of the boom significantly. Therefore a further optimization of the layup and design of the tail end might lead to a boom that performs even better in the performance equation. This research did not investigate the ultimate strength of the boom which might be an option for future work. In this research the ultimate strength of the boom was not elaborated as the FEM results showed stresses that were much lower than the critical stress. However, during crashes different load cases might occur which might lead to different stress zones.

Appendix A

Appendix

A-1 Arduino calibration measurement equipment

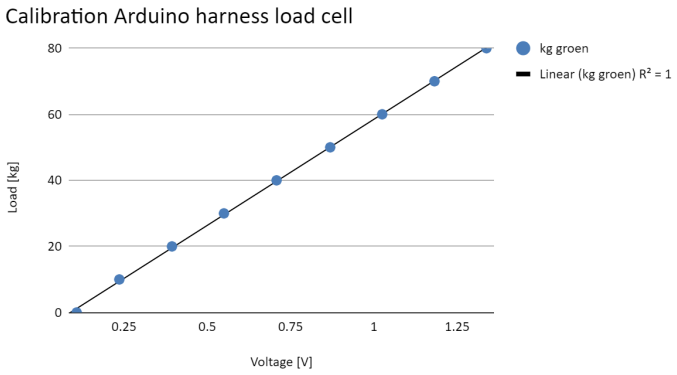

Figure A-1: Calibration Arduino harness load cell

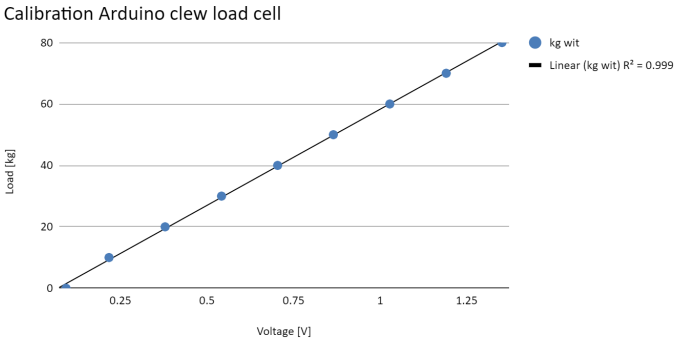

Figure A-2: Calibration Arduino clew load cell

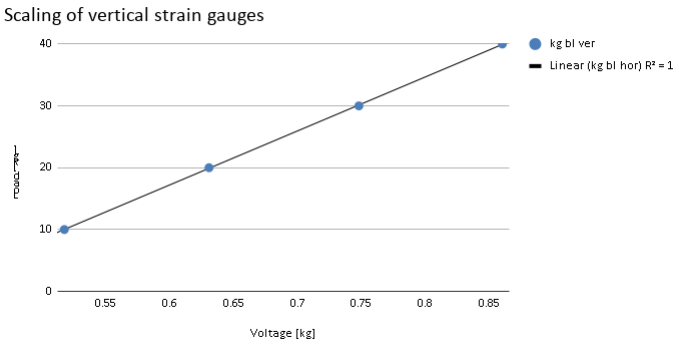

Figure A-3: Scaling of vertical strain gauges

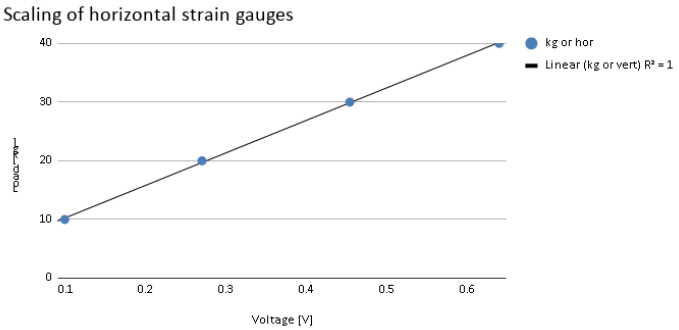

Figure A-4: Scaling of horizontal strain gauges

A-2 Solidworks Interface

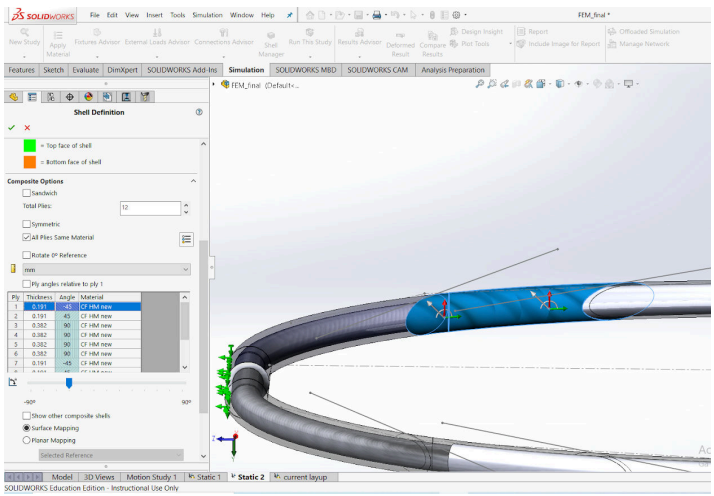

Figure A-5: Example of Solidworks user interface to determine fiber layup

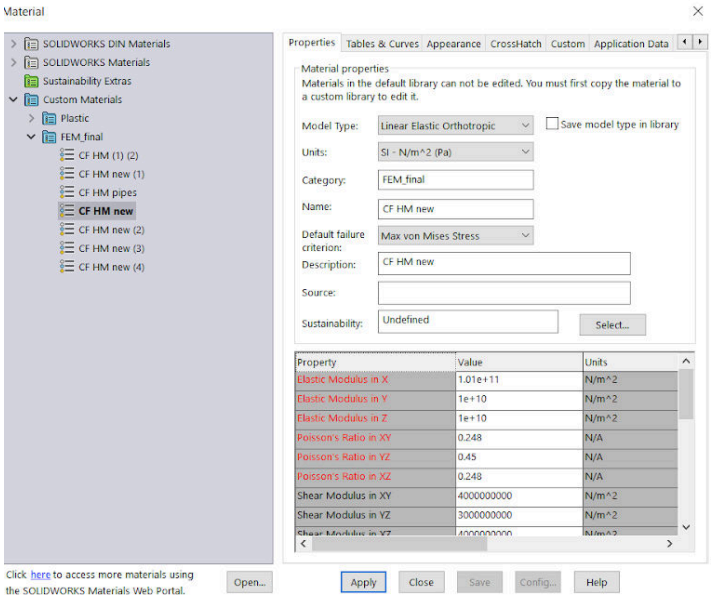

Figure A-6: Example of Solidworks materials menu for orthotropic material

A-3 Layup data

Table A-1: Layup data

Mass	Max displacement lc1	Tail displacement lc1	Horizontal displacement lc2
2.19	21.6	5.08	13.37
2.29	20.0	4.69	12.36
2.35	19.4	4.56	12.00
2.33	19.5	4.59	12.09
2.34	19.6	4.60	12.12
2.37	19.2	4.51	11.89
2.33	19.5	4.59	12.09
2.33	19.3	4.54	11.96
2.36	19.1	4.49	11.83
2.36	19.1	4.49	11.83
2.33	19.3	4.54	11.96
2.31	19.4	4.56	12.02
2.31	20.0	4.69	12.36
2.37	18.7	4.40	11.6
2.39	18.5	4.34	11.43
2.32	19.6	4.60	12.13
2.4	18.5	4.34	11.43
2.35	19.4	4.56	12.00
2.39	18.7	4.38	11.55
2.18	20.6	4.85	12.77
2.25	19.5	4.58	12.06

Continued on next page

Table A-1 – continued from previous page

Mass	Max displacement lc1	Tail displacement lc1	Horizontal displacement lc2
2.16	20.1	4.71	12.42
2.19	19.8	4.65	12.24
2.21	19.6	4.60	12.12
2.22	19.5	4.57	12.04
2.20	19.7	4.63	12.19
2.27	19.3	4.53	11.93
2.30	19.2	4.50	11.86
2.23	19.6	4.61	12.15
2.25	19.9	4.68	12.32
2.26	19.8	4.64	12.23
2.30	19.4	4.56	12.01
2.28	19.5	4.58	12.06
2.22	19.5	4.57	12.04
2.24	19.3	4.53	11.94
2.26	19.1	4.50	11.85
2.29	21.6	5.08	13.38
2.27	22.5	5.29	13.94
2.21	23.0	5.41	14.26
2.27	22.7	5.34	14.07
2.21	21.1	4.97	13.08
2.23	20.6	4.84	12.76
2.27	20.9	4.92	12.96
2.23	20.3	4.76	12.54
2.23	20.1	4.73	12.47
2.27	19.9	4.67	12.31
2.28	19.8	4.65	12.25
2.31	19.4	4.56	12.00
2.25	19.1	4.49	11.81
2.27	19.1	4.47	11.78

Bibliography

[1] "Braided biax sleeve figure." https://www.easycomposites.co.uk/!/fabric-and-reinforcement/carbon-fibre-reinforcement/carbon-fibre-braided-sleeve/carbon-fibre-braided-sleeve-125mm.html), Oct. 2019.

[2] "Unidirectional sleeve figure." https://www.amazon.com/Fibre-Glast-Unidirectional-Carbon-Sleeve/dp/B079MBN8KY, Oct. 2019.

[3] "4 methods for producing composite tubing." https://www.rockwestcomposites.com, Oct. 2019.

[4] "Proboom." https://www.proboom-windsurfing.com/, Oct. 2019.

[5] "What is carbon fiber." http://zoltek.com/carbon-fiber/what-is-carbon-fiber/, Oct. 2019.

[6] "Carbon fiber." http://www.madehow.com/Volume-4/Carbon-Fiber.html, Oct. 2019.

[7] "About prepregs." https://www.fibreglast.com/product/about-prepregs/Learning_Center, Oct. 2019.

[8] "Vacuum infusion guide." https://www.fibreglast.com/product/vacuum-infusion-Guide/Learning_Center, Oct. 2019.

[9] "Carbon fiber: The more you know, the more you can do." https://opedge.com/Articles/ViewArticle/2013-07_10, Oct. 2019.

[10] L. Stangler, "The effects of carbon fiber misalignment on composite material strength." https://openprairie.sdstate.edu/cgi/viewcontent.cgi?article=1685context=etd, Oct. 2019.

[11] "Mechanical properties of carbon fibre composite materials, fibre / epoxy resin (120c cure)." http://www.performance-composites.com/carbonfibre/mechanicalproperties.asp, Oct. 2019.

[12] "Gurit prepreg brochure." www.gurit.com, Oct. 2019.

[13] "Wheatstone bridge figure." https://en.wikipedia.org/wiki/Wheatstone_bridge, Oct. 2019.

[14] "Wheatstone bridge circuit and theory of operation." https://www.electronics-tutorials.ws/blog/wheatstone-bridge.html, Oct. 2019.

[15] "Defining composite shells." https://help.solidworks.com, Oct. 2019.

[16] A. Asadi, "A comparison of cfrp composite laminated joints." https://www.researchgate.net/publication/326034572, Oct. 2019.

[17] H. Jin, "Mechanical strength of composites with different overlap lengths." https://www.osti.gov/biblio/1488647, Oct. 2019.